INVESTIGATIONS INTO THE VARIATION OF THE INTERNAL BALLISTICS OF A SOLID FUEL RAMJET THROUGH COMBUSTOR DESIGN

Charles Ernest Jones

NAVAL POSTGRADUATE SCHOOL
Monterey, California

THESIS

INVESTIGATIONS INTO THE VARIATION OF THE INTERNAL BALLISTICS OF A SOLID FUEL RAMJET THROUGH COMBUSTOR DESIGN

by

Charles Ernest Jones, III

Thesis Advisor: David W. Netzer

Investigations into the Variation of the Internal Ballistics of a Solid Fuel Ramjet through Combustor Design

by

Charles Ernest Jones, III
Lieutenant, United States Navy
B.S., United States Naval Academy, 1966

Submitted in partial fulfillment of the
requirements for the degree of

MASTER OF SCIENCE IN AERONAUTICAL ENGINEERING

from the

NAVAL POSTGRADUATE SCHOOL
September 1973

ABSTRACT

An experimental investigation of the internal ballistics of solid fuel ramjets was conducted in order to more adequately define the pertinent variables in combustor design. The experimental investigation included the effects of wall mass addition on the recirculation zone of a rearward facing step combustor design, various methods of combustor flame stabilization, and the effects of inlet turbulence on the internal ballistics of the combustor.

Flow conditions within the recirculation zone were unaffected by varying rates of wall mass addition.

Swirl devices and centerbodies were found to be inadequate substitutes for the rearward facing step inlet.

The solid fuel ramjet combustor was found to be highly susceptible to inlet turbulence. Smooth inlet ducting 45 degrees off centerline provided nearly identical flame stabilization characteristics and regression rates as that of a previously designed axial inlet configuration.

TABLE OF CONTENTS

LIST OF FIGURES

LIST OF TABLES

ACKNOWLEDGEMENTS

The author wishes to express his appreciation to Associate Professor David W. Netzer of the Department of Aeronautics for his guidance, encouragement, and assistance throughout the project.

Appreciation also goes to Patrick J. Hickey, Jr. and Edward Michelsen who, with the remainder of the technical staff of the Aeronautics Department, furnished timely and efficient technical assistance.

This work was sponsored by the Naval Weapons Center, China Lake, California under Work Request 2-3044.

I. INTRODUCTION

The solid fuel ramjet refers to a propulsion system consisting of solid fuel and ambient air as the oxidizer. While possessing many of the characteristics of solid fuel rockets, the solid fuel ramjet does not have the weight penalty of carrying its own oxidizer. This feature is extremely attractive to the design engineer investigating ways of increasing the tactical range of missiles. An additional advantage can be achieved in handling safety and storage due to fuel-oxidizer separation. A feasible design configuration is shown in Figure 1.

Although solid fuel rockets have been used for many years, a complete understanding of the combustion mechanism(s) has not been achieved. While there are several models available making use of different driving mechanisms to achieve combustion, most performance calculations are based upon empirical formulae developed through experimentation. The recent interest in hybrid rockets (systems using solid fuel and liquid and/or gaseous oxidizer) has resulted in the development of even more difficult combustion analysis /Ref. 1/.

While the solid fuel ramjet is commonly classified as a hybrid rocket, it lacks two of the major characteristics of hybrids. In general, hybrids operate under high chamber pressures, much as do solid fuel rockets. This feature, along with relatively low oxidizer mass flow rates, permits

flame stabilization to be achieved within the chamber boundary layer. In contrast, the solid fuel ramjet must operate at relatively low chamber pressures and high oxidizer flow rates. Such conditions greatly dilute the fuel-air mixture and prevent normal boundary layer flame stabilization.

In October, 1971, the Naval Postgraduate School (NPS) inititated a study of the internal ballistics of solid fuel ramjets. This study was to coincide with research and development efforts of the Naval Weapons Center, China Lake; the Air Force Aero Propulsion Laboratory, Wright-Patterson AFB; and the United Technology Center (UTC), Sunnyvale. The objectives of the NPS research program centered around the development of an analytical computer model designed to predict blow-off limits for the solid fuel ramjet combustor. Peripheral areas of investigation included methods of flame stabilization, the effects of inlet flow distortion on the combustion, and the functional dependence of regression rate on design parameters.

In early 1971, UTC found that a sudden expansion inlet (also known as the rearward facing step design) would sustain combustion in a solid fuel ramjet (Figure 2) /Ref. 2/. For this reason, the computer model selected for investigation at NPS was Spalding's PISTEP II program which solved for heat and mass transfer in a recirculating flow using a finite difference method /Ref. 3 and 4/. The model was to be extended to include wall mass addition and combustion. Experimental data were then to be used to verify the computer solutions.

The initial investigation at NPS was conducted by L. D. Boaz [Ref. 5]. His efforts centered around three specific areas. Using an axisymmetric non-reacting flow, he visually observed the recirculation zone adjacent to the step inlet (Refer to Figure 2). From these observations he was able to conclude that the size of the recirculation zone and the location of the reattachment point depended on the step height ratio (h/D) but were independent of inlet velocity. In addition, Boaz extended PISTEP II to include wall mass addition. Computer solutions analytically predicted that wall mass addition would have little effect on the size of the recirculation zone or the location of reattachment. He did not, however, prove this experimentally. Boaz's third area of study was concerned with the functional dependence of regression rate on configuration and test environment. He found that the average regression rate was a specific function of chamber pressure, inlet air temperature and average mass flux of air. Maximum regression occurred near the reattachment point location and thereafter decreased slightly with increased distance from the head end. The data indicated that the average regression rate closely followed the theoretical expression derived for kinetically-controlled hybrid rocket combustion. This result offered validity to the assumption that the solid fuel ramjet behaves as a pressure sensitive hybrid rocket combustor downstream of the reattachment point.

Additional information is necessary to more fully understand the flame stabilization in solid fuel ramjets. Because

of the flight environment facing the solid fuel ramjet, the air or gas flow rate entering the combustion chamber is greater than the turbulent flame speed. A similar situation exists in turbojet and liquid fuel ramjet combustors. Successful flame stabilization has been achieved in those combustors through the use of bluff bodies such as V-gutters, strips, rods, and centerbodies (Figure 3) [Ref. 6]. The fuel and oxidizer are generally premixed forward of the bluff body. Combustibles existing in the recirculation zone are initially ignited from an external source. In the recirculation zone, fresh combustibles enter and are burned and cause a high wake temperature. This action ignites the free stream gases as they pass over the body, and a flame front is formed [Ref. 7].

The stabilization devices mentioned above all use liquid fuel. Blow-off limits are dominated by the particular injector design and inlet conditions. The transformation of solid fuel into vapor for combustion is normally accomplished by heat, implying that the category of stabilizers discussed above may not be directly applicable to solid fuel ramjets. An effective combustion design for the solid fuel ramjet must include three items similar to liquid fuel combustors:

1. The particular flow pattern must ensure that hot gases or high temperatures are in close proximity to the fuel grain to cause sublimation.

2. The vaporized fuel must be mixed in proper proportions to permit combustion.

3. The flow rate of the combustible mixture must be equal to or slower than the turbulent flame speed at a location ahead of the expected flame front.

Practically any flame holder design will work if the inlet gas velocity is reduced to at or below the turbulent flame speed. However, because large pressure losses are incurred in velocity reductions, the stabilization method plays a major role in combustor performance and efficiency.

The objectives of this present thesis were to experimentally investigate the effects of wall mass addition on the recirculation zone, additional flame stabilization methods, and the effects of inlet turbulence on the internal ballistics of the combustor.

Figure 1 shows one particular configuration tested. The ducting design should be based upon conservation of space and weight. No previous investigations have been conducted on the effects of non-axial inlet ducting on solid fuel ramjet combustion characteristics. Turbulence and inlet distortion are important parameters in air breathing engines where smooth inlets are, in general, a necessity. Aside from possible changes in regression rate, the blow-off limits for solid fuel ramjets may also be susceptible to inlet flow characteristics.

II. METHOD OF INVESTIGATION

Non-reacting flow visualization tests were conducted using a two-dimensional, planar model of the rearward facing step design with inert gas wall-blowing downstream of the steps. The two-dimensional design facilitated the use of schlieren photography to record flow phenomena. (However, it was understood from the findings of Abbott and Klein [Ref. 8] that there were certain inherent disadvantages in the two-dimensional, planar configuration, foremost of which was non-symmetrical axial flow.)

Schlieren photography recorded the vertical variations of density created by heat, velocity, and molecular weight gradients. A similarity to the reacting flow tests conducted by Boaz [Ref. 5] was achieved by matching air mass flux and wall gas mass flux (See Appendix A).

The effects of wall mass addition and inlet distortion on flow characteristics and the reattachment point were measured qualitatively for the rearward facing step design. The flow characteristics of a centerbody design were also investigated with wall mass addition included.

Two devices were investigated as possible flame stabilzation alternatives to the rearward facing step design. These included a centerbody and a swirl device. The centerbody design can be classified as a bluff body (which has already been discussed). The swirl device was seen as a possible method

to reduce the axial velocity components of the gases to a value below the turbulent flame speed. While tangential velocities were greatly increased, gas contact time was greatly extended and stabilization may be expected to result. These stabilization devices were tested in reacting flows using a cylindrical combustor with plexiglas as the fuel.

The final area of investigation dealt with inlet ducting. Reacting flow tests with the plexiglas grain were conducted, and blow-off limits were determined. Observations were made of the effects of flow straighteners ahead of the inlet. Inlet ducting of 90 degrees and 45 degrees off the combustor axis were tested.

III. DESCRIPTION OF APPARATUS

A. NON-REACTING FLOW VISUALIZATION APPARATUS

A schematic of the flow visualization apparatus showing the overall system is presented in Figure 4. Figures 5 through 8 are photographs of the apparatus.

1. Test Apparatus

The test apparatus consisted of three major sections -- a converging section, a straight section, and a test section (Figure 9).

Air flow entered the converging section from a plenum chamber through a sonic choke plate and diffuser plate. The diameter of the sonic choke was 0.681 inches. The area contraction ratio in this 9.5-inch section varied, depending upon the size of the step inserts used. For the 1/2-inch step nominal case, the area contraction ratio was 16.

Following the convergence section, a straight section of 10.5-inch length was used to achieve fully developed flow. The height of the step could be varied by using different inserts: 3/8-inch, 1/2-inch, or 5/8-inch. The 1/2-inch steps were predominantly used in this investigation.

A test section of 10.5 inches in length was available although only 6.67 inches of it were externally visible. Porous bronze plates were used at the top and bottom of the section for the first 6.75 inches. Inert gas was brought into plenum chambers directly behind the plates and blown into the test section to simulate wall mass addition. Following the test section,

all flow was vented to the atmosphere.

2. Air and Inert Gas Supply

A Sullivan air compressor delivered air at pressures up to 300 psig to a 2000-cubic foot reservoir. A main air valve was used to regulate inlet mass flow rates. Auxiliary air provided flow to the heater unit until the desired temperatures were reached in the secondary flow.

Bottles of inert gas (helium and argon) were connected in parallel and provided secondary flow through the porous bronze plates. Secondary gas flow was controlled with a flow regulator. The gases were directed through a heater and then into a secondary chamber (stainless steel, I.D. = 2.053 inches) containing a sonic choke plate. Hole diameters of 0.205 and 0.109 inches were used to choke the helium and the argon gas flows respectively.

3. Heating System

The heating system consisted of 3/8-inch copper tubing coiled in an asbestos-lined steel container. An A.C. arc welder capable of delivering up to 200 amps was connected in such a way as to provide a circuit through the coil of copper tubing. Gas flow temperatures on the order of 200 degrees F. were used. Temperatures in excess of this were expected to be detrimental to the test apparatus. The length of the 3/8-inch copper tubing between the secondary chamber and the test section was kept to a minimum to avoid heat loss.

4. Data Acquisition System

Pressure measurements were taken from the main plenum

chamber and the secondary chambers. Two Heise pressure gauges having scales of 0-300 psig were used to provide readings. Galvanometers were used to measure the two iron-constantan thermocouple outputs. One thermocouple was located in the main plenum chamber, and the other ahead of the sonic choke in the secondary chamber.

5. Peripheral Equipment (Figure 10)

Fine and coarse screens were used in the latter portion of the investigation to study the effects of inlet turbulence on the flow characteristics within the recirculation region. Small channels were cut into the 1/2-inch step inserts approximately 3/4 inch upstream of the inlet to permit installation of the screens. When not in use, the slits were covered with smooth tape.

A two-dimensional centerbody was also used. Support equipment for the centerbody required the use of 1/8-inch step inserts and 1/16-inch copper wire (see Fig. 10).

6. Schlieren Apparatus

A standard black and white schlieren set-up was used. A Polaroid camera was used to record flow conditions.

B. REACTING FLOW APPARATUS

A schematic of the solid fuel ramjet apparatus showing the overall system is presented in Figure 11. More specific details are presented in Reference 5.

1. Motors

The general configuration of motors can be broken down into four sections -- head end assembly, step insert

section, grain, and aft closure. Figure 12 shows the total assembly as used by Boaz. All metal parts except for bolts were made of stainless steel. Pressure and temperature measurements were taken in the head end assembly, and one additional pressure measurement was taken at the aft closure section.

Modifications to the head end assembly and step insert section are shown in Figures 13 and 14. No modifications were made on the grain or aft closure sections.

Three head end assemblies were used -- axial, 90 degrees, and 45 degrees. Measurements of inlet pressure and temperature could be made on all assemblies except for the 45-degree configuration.

Two step insert sections were used, accommodating either a long step insert or a short one (Figure 15). A centerbody design and a swirl design could be used interchangeably with the long step insert.

The centerbody insert consisted of a solid cone suspended by four 1/16th-inch wires. The wires were initially stainless steel but were later changed to tungsten. The base of the centerbody was 1.146 inches in diameter, and its height was one inch. The insert shell had an inner diameter of 1.25 inches which provided a 0.125 step upon entrance into the grain section.

The swirl insert consisted of four symmetrical airfoils connected to a 0.312-inch diameter hub. The airfoils were set at a 30-degree angle to the flow and supported by

stainless steel pins. Two devices were constructed in such a way as to provide either a 0.187-inch step or a 0.312-inch step upon entrance into the grain section.

Although a variety of long step inserts was available, tests in this investigation were only performed with the 0.5-inch diameter insert. Only one short step insert was constructed having a diameter of 0.5 inch.

2. Inlet Ducting

Four different inlet ducting configurations were used. A straight 1.5-inch pipe was used for the axial inlet motor configuration. One pipe contained 2.0-inch flow straighteners, and one did not. For the 90-degree motor, 1.0-inch pipe was used without flow straighteners. Figure 14 shows the inlet ducting for the 45-degree motor configuration. Flow straighteners and smooth, thin-wall stainless steel tubing were incorporated in this design.

3. Ignition System

Two different ignition systems were used, although each incorporated an oxygen-methane mixture ignited by a spark plug. The axial inlet and 90-degree inlet configurations had two ports for oxygen and two for methane with entry made slightly ahead of the step inserts. The mixture was then ignited with two spark plugs (Figure 13).

An alternate system was employed on the 45-degree inlet configuration. An external chamber was used to mix and ignite the oxygen and methane. The resulting flame was then directed into the head end assembly (Figure 14).

4. Gas Flow System and Control

The gas flow system remained essentially the same as that used by Boaz. Non-vitiated air was received from the compressor at pressures to 150 psia. Although an air heater was available, it was not used in this investigation (Figure 11).

A standard ASME orifice flow meter was used to measure air flow rates entering the motor. A manually-operated gate valve located between the flow meter and motor was used to set the desired flow rates. Two pneumatically-operated Jamesbury ball valves operated synchronously to allow either the air flow to enter the motor or be vented into the test cell.

A nitrogen purge and cooling air system were connected upstream of the head end assembly and were controlled by electrical valves. The nitrogen purge system operated for approximately one second to extinguish the combustion flame following a hot firing run. Cooling air from a low pressure supply was then blown through the motor as necessary.

A secondary ASME orifice flow meter was constructed to be used in connection with certain inlet ducting configurations. However, the system was never put into operation.

5. Data Acquisition System

Pressure transducers included a Colvin 0-35 psi differential transducer to measure the pressure drop across the orifice flow meter and three Wiancko 0-200 psig transducers to measure orifice pressure, motor inlet pressure, and chamber pressure.

Two iron-constantan thermocouples were used to measure the temperature at the flow orifice and the temperature at the head end assembly. Thermocouple measurements were recorded on a calibrated 0 to 600-degree F. strip chart recorder.

A Honeywell Model 2106 Visicorder was used to record all pressures, an ignition pulse, and a timing signal.

IV. EXPERIMENTAL PROCEDURE

A. NON-REACTING FLOW TESTS

The non-reacting flow tests were performed at the gas dynamics laboratory of the Naval Postgraduate School. Schlieren photographs were obtained for various inlet velocities, molecular weights of wall blowing gas, and temperatures of the gases entering the test section.

Air mass flow rates were chosen to conform to the high and low values used in reacting flow experiments where normal operation was expected to occur. Normal operation implied a mass flow rate of between 0.10 and 0.22 lbm/sec. in reacting tests. This yields to air flux rates (G) of between 0.0566 and 0.124 lbm/sec-in^2. In the discussion below, the term "high inlet" refers to values of G equal to about 0.124 lbm/sec-in^2, and "low inlet" to values of approximately 0.0566 lbm/sec-in^2 (See Appendix A).

An identical method was used for obtaining similarity between average regression rates of reacting flows and wall mass addition rates. Average regression rates varied between 0.005 and 0.0117 in/sec in reacting tests. Therefore, "low blowing" was defined as G values of about 0.000177 lbm/sec-in^2, and "high blowing" as values in the neighborhood of 0.000637 lbm/sec-in^2.

To ensure that density gradients were visibly present, blowing gases of argon and helium were used. Heating the helium

gas increased the density gradients and provided better visual patterns. Heating was not used with the argon as it reduced density gradients with the inlet air. Because of the configuration of the heater unit, auxiliary air flow was first heated to desired run temperatures, and then helium flow replaced the air flow during the run.

The investigation was to include the collection of data from three different step inserts -- 3/8-inch, 1/2-inch, and 5/8-inch. It was found that the recirculation zone of the 3/8-inch step insert was too small to be of value for schlieren operations. The 1/2-inch step inserts were then chosen as a nominal case because of their similarity to reacting tests to be performed later. The 5/8-inch step insert was never used.

Following a complete series of tests that included various combinations of inlet conditions and wall mass addition rates using helium, the blowing gas was changed to argon. Repeatability was checked on each series.

A series of tests was then made using the screens (Figure 10) to induce different levels of turbulence. Finally, the centerbody design was investigated in a series of tests.

A record of each run was made by taking a Polaroid picture of the test section through the schlieren. While schlieren alignment was done before each series of runs, focus and contrast had to be adjusted during each run.

B. REACTING FLOW TESTS

The reacting flow tests were performed in the jet engine test cell at the Naval Postgraduate School. Ten different

versions of inlet ducting, head end assembly, and step insert sections were investigated. Nominal conditions when applicable are summarized in Table I.

TABLE I

NOMINAL TEST CONDITIONS

Chamber pressure (psia) (Nozzle diameter = 0.747 inch to achieve chamber pressure)	60
Inlet diameter (in)	0.5
Inlet temperature (Degrees F.)	65
Air flow rate (lbm/sec) (Air flux = 0.11 lbm/sec-in^2)	0.20
Grain length (in)	12
Step (h/D)	0.333

Each different motor version was tested for blow-off limits. Flow conditions were set by monitoring the differential pressure (delta P) across the ASME orifice flow meter. A mass flow rate of 0.165 lbm/sec (G=0.093 lbm/sec-in^2) was achieved with a delta P = 10 psi. Delta P was varied between zero and 30 psi to locate conditions where combustion was self-sustaining.

During the blow-off tests, run time generally included three seconds of ignition, two seconds of ignition plus air flow, and three seconds of self-sustaining combustion with only air flow prior to a nitrogen purge. Such a schedule facilitated the use of one grain for several runs.

There were three possible outcomes for each run: 1) Following ignition termination, combustion was sustained; 2) following ignition termination, combustion was not sustained; or 3) upon initiation of main air, ignition was terminated. The first two cases deal with blow-off limits; whereas, the third involves the ignition system design and offered no information on blow-off limits.

Repeatability was tested often, especially on non-sustaining runs. Ignition times were lengthened in some cases to ensure non-sustaining runs were not affected by increased ignition times.

Following the series on blow-off limits, full 30-second test runs were made on the sustaining combustor designs that were considered markedly different from Boaz's motor configuration. Repeatability was checked, and a test made with Boaz's motor to check agreement with past data.

V. RESULTS AND DISCUSSION

A. NON-REACTING FLOWS

1. Method of Analysis of Schlieren Photographs

All photographs were taken with a horizontal knife edge which implies density gradients will only be visible in the vertical direction. Unless otherwise indicated (i.e., "reversed knife edge"), the positive y direction is taken from the bottom of the photograph to the top. Visible contrast is proportional to the first derivative of density with respect to y. Therefore, if density is increasing in the positive y direction, contrast, or lighter tones, will be encountered in the positive y direction.

Assuming the perfect gas law applies to air and inert gases such as helium and argon, density is proportional to static pressure (p) and molecular weight (m) and inversely proportional to absolute temperature (t).

The variation of static pressure in the y direction was considered negligible. Using isentropic relations and the perfect gas law, static temperature becomes inversely proportional to flow velocity squared.

These assumptions are considered quite adequate for the qualitative effects desired in this investigation. Table II summarizes the flow properties affecting contrast (increased white) on the schlieren photographs.

TABLE II

FLOW PARAMETERS AND THEIR EFFECTS ON SCHLIEREN CONTRAST

Contrast or $\partial\rho/\partial y$	Standard Knife Edge			Reversed Knife Edge		
	$\partial m/\partial y$	$\partial t/\partial y$	$\partial V/\partial y$	$\partial m/\partial y$	$\partial t/\partial y$	$\partial V/\partial y$
Increases if	inc	dec	inc	dec	inc	dec
Decreases if	dec	inc	dec	inc	dec	inc

2. Orientation of Photographs

Reference is made to Figure 16. The upper and lower steps, 0.5-inch high in this case, can be seen at the far left with air flow entering between the two steps. Fluid flow is from left to right. The upper and lower surfaces are porous bronze plates through which the inert gas can be blown uniformly.

The black object in the center of each photograph is an access hole through the glass side plates. The hole was covered with tape to prevent possible disruption of the flow. Because of the critical nature of glass distortion on schlieren photography, these glass plates were the best available.

It may be noted some of the photographs exhibit solid lines that appear to conform to the flow. The lower left-hand corner of Figure 14 shows such a line. These lines were caused by condensation on the windows during the run.

Although particular care was taken to ensure proper alignment of the schlieren system, the photographs show the camera to be slightly off alignment as indicated in the following figure.

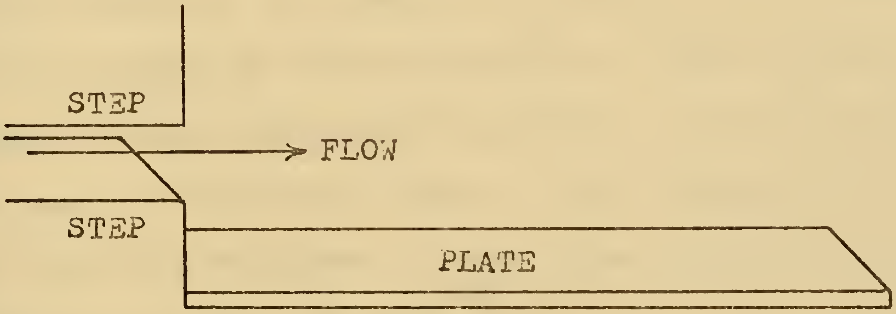

It should be mentioned that all photographs in this report have been expanded to approximately 135% of normal size.

3. No Mass Addition
(Figures 16, 17, and 18)

The basis for comparing the effects of blowing on flow characteristics must be taken from photographs in this group having no mass addition. Figures 16 and 17 show typical views of low and high inlet flows respectively. Figure 18 is provided to show how shock patterns will form at higher G levels.

G levels on the order of 0.06 to 0.08 are considered as "low" inlet conditions. G levels near 0.09 are classified as"medium" inlet conditions, and those from 0.11 to 0.13 are called "high" inlet conditions for purposes of this investigation.

The density gradients in this grouping are primarily created by velocity gradients that in turn affect temperatures. The small white circular area in the upper-left-hand corner of Figure 17 is thought to result from a secondary vorticity created by the reverse flow. Such phenomena are observed in later photographs as well. A thin boundary layer can be seen on the bottom plate. When viewing later photographs, one must "subtract" these items in order to examine the effects of wall mass addition.

One final point should be mentioned here. All photographs in this group show what can be classified as a "short" reattachment to the bottom plate. Abbott and Kline /Ref. 8/ demonstrated that in two-dimensional planar flows, a long and a short reattachment exist on alternate sides. In this investigation, the side receiving the short reattachment could not be predicted. Test section orientation seemed to have no effect. Most of the runs made in this investigation resulted in the short attachment being located on the bottom plate, and the long attachment on the top plate far downstream and out of view.

4. Wall Mass Addition with Heated Helium (Figures 19 through 27)

The investigation was initially set up to gather data on three different inserts. It was felt that the reattachment location could be accurately measured from the photographs taken. Figures 19 and 20 were tests made on the 3/8 inch steps. The small size of the recirculation zone made determination of the reattachment point difficult. The switch was then made to the 1/2-inch step to achieve a larger recirculation zone. As testing continued, it was felt more could be achieved by using only one step and varying other parameters. Consequently, the 5/8-inch step insert was never used.

A grid system was used on the 3/8-inch step test but abandoned thereafter because of increased visual distortion of the flow through the additional plastic grid.

Heated helium was used in all of these tests. Helium temperature varied slightly from run to run; however, 140 degrees F. was the approximate average. Low blowing rates were considered to be values of G near 0.00024 lbm/sec-in^2. All short reattachments were made on the bottom plate.

The division of flow at the reattachment can be seen relatively well on the bottom plate. The exact location of the reattachment point should be where the boundary layer is thinnest. Measurements of this point were susceptible to large errors because of the relatively flat boundary layer profile within the area of interest. For this reason, actual

measurements of the reattachment point made from the photographs were deleted from this investigation. However, certain qualitative results were obtained.

The backflow to the left of the reattachment point appears to enter a highly turbulent area near the step where density gradients are quite high. The high gas concentrations, which in a reacting flow would be fuel, appear to join the main inlet stream just aft of the step.

The dark zone slightly above and left of the reattachment point appears to be of uniform density. This could suggest either the possibility of a "well-mixed" area of air and helium or an area of low velocity within the "center" of the recirculation zone.

It can be seen that the size of the boundary layer is dependent upon inlet mass flow rates as well as on wall mass addition flow rates. Figure 26 was an attempt to obtain better clarity of the gradients in the upper portion of the test section. Although unsuccessful in showing detail, it quite vividly depicts the lack of symmetry in two-dimensional planar flows.

This grouping of photographs would suggest the flame stabilization mechanisms are not much different from those encountered in bluff body stabilization. In an axisymmetric system, the step would represent a continuous version of one side of a bluff body. Initially an ignition system drives hot inlet gases over the step. Some of the gases continue downstream, while others reverse their flow at the reattachment point and travel toward the step. Heat given off by these

gases sublimate the fuel from the grain. This hot fuel vapor is mixed with the air as it travels up the step face and then along the dividing streamline. Ignition takes place, and a flame front propagates downstream. Some of the hot products are recirculated to continue the process.

In general, a point is reached for a particular configuration where the inlet mass flow rates are too high to permit flame stabilization. Several models have been used to explain flame stabilization regions and define the mechanisms controlling blow-off limits (ignition vs. contact time, mixture ratios, etc.). Flame blow-offs may also be created by turbulence.

The helium blowing photographs allowed good visual observations to be made. It was expected that the higher blowing rates might change the characteristics of the recirculation zone. Such appeared not to be the case -- at least with the magnitude of blowing used in this investigation. From the qualitative measurements that could be taken, the location of the reattachment point seemed very stable and unaffected by the blowing and/or the inlet velocities.

5. Wall Mass Addition with Unheated Argon (Figures 28 through 35)

To investigate the effect of fuel molecular weight on the blowing behavior, argon (molecular weight of 40) was used in place of helium.

In this series of tests, the location of the short reattachment point varied from run to run. No explanation could be found for this behavior. Density gradient patterns were

very similar to those seen with helium blowing; however, visual analysis was more difficult. The lack of visual clarity can best be explained by the effects of velocity and molecular weight negating one another in the schlieren photographs.

It was concluded from these runs that no appreciable change was made in the characteristics of the recirculation zone by changing the blowing gas from a light molecular weight to a heavier one.

6. Induced Turbulence with Heated Helium (Figures 36 through 45)

This series was conducted to determine the effects of inlet turbulence on the recirculation zone.

At low and medium inlet conditions, the fine screen did little to alter the characteristics of the recirculation zone (Figures 36 and 37). However, at high inlet conditions (Figures 38 and 39) the characteristics were significantly changed. The flow seemed completely disrupted in that a well-defined recirculation zone was no longer present.

With the coarse screen, disruption took place under all inlet conditions. It was first believed that the short reattachment location had moved to the upper plate, and the recirculation zone was similar to previous findings. Figure 44 suggested such was not the case. Helium was not being collected in sufficient quantities to create high density gradients near the step. The "well-mixed" or uniform velocity zone became greatly exaggerated.

A check on the effects of increased blowing in Figure 45 revealed it had little effect on the inlet turbulence.

From this test series, it appeared that the characteristics of the recirculation zone were very susceptible to inlet turbulence. This would indicate that the blow-off limits may also be caused by a disruption or a loss of the recirculation zone because of inlet turbulence. These results indicate solid fuel ramjet combustion may be highly susceptible to high inlet turbulence levels.

7. Centerbody with Heated Helium (Figures 46 through 52)

Since centerbodies had been used successfully in liquid fuel ramjets, such designs might also have applications for the solid fuel ramjet. If sufficient amounts of fuel are able to gain access to the recirculation zone behind the centerbody, flame stabilization would occur. Two-dimensional flow visualization offered an opportunity to see how the fuel would mix with the inlet air flow.

Results indicated recirculation zones containing fuel (helium) attached behind the 1/8-inch steps. Although a recirculation zone did follow the centerbody, it appeared little or no fuel was permitted to enter this area. These results indicated that little or no success would be gained from a centerbody design under reacting test flow conditions. Reacting tests were scheduled to verify this.

B. REACTING FLOW TESTS

Data from these tests are summarized in Appendix B, "Blow-Off Limit Data" and Appendix C, "30-Second Hot Firing Data".

1. Axial Inlet Ducting Blow-Off Limits

The first inlet ducting system employed was the axial configuration used extensively by Boaz [Ref. 5]. Motor Configuration A (from Ref. 5) was initially tested to ensure the system was working properly and correlations could be made between earlier findings and those of this investigation. Sustained combustion was obtained on every test using the nominal conditions previously listed on page 26 and varying air mass flow rates. Such findings were in agreement with the work done by Boaz.

Although the motor used by Boaz was well designed to perform reliable regression rate tests, the inlet was considered too large to be of significant value in the flyable design of a solid fuel ramjet. The goal was set to test the limitations of that design and to construct as small a motor inlet as practical.

A series of tests were made to see what effect a reduction in the length of the 1/2-inch step insert might have on flame stabilization. A full range of mass flow rates was investigated using Motor Configuration B, and no detrimental effects were observed. It was concluded that the short step insert offered the same performance characteristics as the long one.

The test rig used by Boaz included flow straighteners immediately downstream of one of the Jamesbury ball valves (see Fig. 11). Although it was believed these straighteners were necessary for obtaining repeatable data, an actual

investigation into their value had never been undertaken. The next step, then, was to remove the straighteners to see what effect they had on flame stabilization.

Results showed that up to a certain air mass flux ($G = 0.102$ lbm/sec-in^2), combustion was normal. However, above this level the ignition system blew out when main air was vented into the motor.

The flow straighteners were reinstalled, and tests were begun on the alternate flame stabilization devices. The first one tested was the swirl device with a 5/16-inch step. It was felt that the greater the step size, the more likelihood of success.

Three tests were run at very low mass flux rates before excessive "spark levels" were noted leaving the exhaust. No sustained combustion had been achieved to that point. Upon investigation for the spark source, it was found the ignition system was melting the leading edges of the swirls' stainless steel airfoils. Tests with the swirl device were terminated because: 1) It was felt the data were sufficient to indicate the device was not an adequate substitute for the rearward facing step design, and 2) it was not considered desirable to redesign either the ignition system or rebuild the swirl devices to sustain higher temperatures considering the expected results.

The centerbody was tested next. The total air flow area around the centerbody was equal to the area seen by the air through a 1/2-inch step. After three unsuccessful attempts

to achieve sustained combustion, the motor fired successfully for 3.5 seconds before shut-down and a nitrogen purge. Upon inspection, it was found that three of the four stainless steel struts had burned through. The centerbody had apparently fallen to one side and permitted a much larger hole to be exposed. Since the centerbody was in good working order (no melting or deterioration), the struts were replaced with tungsten rods. Subsequent tests resulted in no ignition below a value of G = 0.085 lbm/sec-in^2 and ignition blow-out above that level. Sufficient information, both from non-reacting and reacting flows, had been obtained to indicate the centerbody design was not feasible.

Both the swirl device and the centerbody had theoretical possibilities; however, upon experimentation, they failed to perform. The investigation into the effects of turbulence discussed above can also help to explain why a combination swirl and step configuration would not work. The step offers a recirculation to the flow, but the added swirl kept the recirculation zone from fully forming. There may be, however, a particular flow angle design for which a swirl device might be able to maintain flame stabilization. The present study cannot be used to verify or disprove that possibility. Considering what has been learned, however, it would seem the added design and construction costs of a swirl device would not make it competitive with the simpler rearward facing step design.

The problem with the centerbody design was also apparent in the non-reacting visualization tests. Insufficient quantities of the wall blowing gas were able to migrate to the

bluff body recirculation zone. Thus, in the reacting flow situation, the fuel-air ratio was too low, and combustion could not be sustained.

2. 90-Degree Inlet Ducting Blow-Off Limits

As previously mentioned, one of the main areas of interest in this investigation was to reduce the overall size of the solid fuel ramjet inlet system. It was shown that an axial inlet worked. The shortest possible total configuration would be to use 90-degree inlet ducting. Tests were conducted to examine this extreme case.

Pipe fittings were used in this configuration without flow straighteners for three reasons: 1) Not all the information had been gathered on inlet turbulence effects before these tests; 2) construction was simple, and any turbulence generated by the Jamesbury ball valve was expected to be dissipated by the time it reached the motor head assembly; and 3) the severe mixing turbulence at the junction of the two inlet streams was considered to be several orders of magnitude greater than any possible turbulence created before or through the inlet ducting.

Tests were made using both the long and short 1/2-inch step inserts to see if they had any effect on reducing the mixing turbulence. Out of nine trials, only one was successful in sustaining combustion, and it was not repeatable under similar inlet conditions. This one success was discarded as unreliable since the grain used had an excessively large port

diameter accrued from many trial runs. It should be pointed out that greater flame stability can be achieved by increasing h/D. Partially burned grains offered better stability than new grains. This investigation concurs with Boaz's findings in this matter.

The lack of success with the 90-degree inlet ducting centers around the excessive turbulent mixing at the junction of the two inlet streams and possibly to a lesser extent the turbulence generated within the ducting itself. Since mixing losses are so high in such a system, rather than improving the ducting system, efforts were spent on a motor with a lower inlet angle.

3. 45-Degree Inlet Ducting Blow-Off Limits

The ducting system was modified to include smooth, one-inch tubing and flow straighteners. The motor itself proved to be the smallest design used. The ignition system was modified to remove the spark plugs and ignition ports. This allowed for a more compact design. Inlet pressure and temperature probes could be installed but were not used.

Test results showed sustained combustion could be achieved at all system flow rates. A check was made into the combustor's performance with one intake duct shut off and full flow coming through the other. Combustion could not be sustained under this configuration. Non-symmetrical inlet flows are common in maneuvering missiles. This area should be investigated in later studies.

4. Comparison of the 45-Degree Inlet with the Axial Inlet

Three 30-second tests were run to see if the regression rates of the 45-degree inlet version differed markedly from Boaz's data on the axial inlet. Appendix C summarizes the results. Two tests were made using the 45-degree inlet to ensure repeatability, and one test was made with the axial inlet to compare with the results reported by Boaz.

Although the 45-degree inlet caused slightly higher average regression rates (based on weight loss) than obtained by Boaz with the axial inlet, the values fell well within the 10% experimental error limits. From this result, it can be assumed the average regression rate formula given previously by Boaz can still be applied.

Figure 52 shows the variation in burning rates along the length of the grain for the two inlet configurations. The 45-degree inlet caused higher regression rates at the head end of the grain; while the axial inlet caused higher regression rates in the aft section. A difference in regression patterns was not unexpected. The two-dimensional schlieren photography indicated inlet turbulence levels tended to modify the flow characteristics of the recirculation zone.

From these tests, it appeared the 45-degree inlet ducting configuration offered the same basic performance characteristics as the axial inlet. Yet, it was significantly shorter and more compact. Further studies will be necessary to compare system and motor efficiencies and specific impulse.

VI. CONCLUSIONS

The non-reacting flow visualization tests showed that the reattachment point location was not a function of the inlet or the wall addition mass flux within the normal flight regimes of a solid fuel ramjet. The lack of dependence on inlet mass flux concurred with Boaz's experimental findings using an axisymmetrical test section. The independence of the reattachment point location on wall mass addition is in agreement with the computer model (PISTEP II) predictions.

Mechanisms involved in flame stabilization of the backward facing step design are quite similar to those present in bluff bodies.

Inlet turbulence affects the blow-off limits by significantly changing the structure of the recirculation zone. Both non-reacting and reacting tests showed inlet turbulence to be a highly significant parameter in the design of a solid fuel ramjet. Significant design efforts must be undertaken to ensure that inlet ducting is smooth and free stream turbulence is adequately dampened before entry into the motor.

Alternate flame stabilization devices, including the swirl and centerbody designs, proved inadequate substitutes for the rearward facing step design. Neither was able to stabilize a flame effectively.

An improvement was made in the design of the solid fuel ramjet by switching to a 45-degree inlet configuration. The

reduction in size and weight from the axial design improved the feasibility of using a solid fuel ramjet motor for missile propulsion. Flame stabilization characteristics and regression rates were nearly identical.

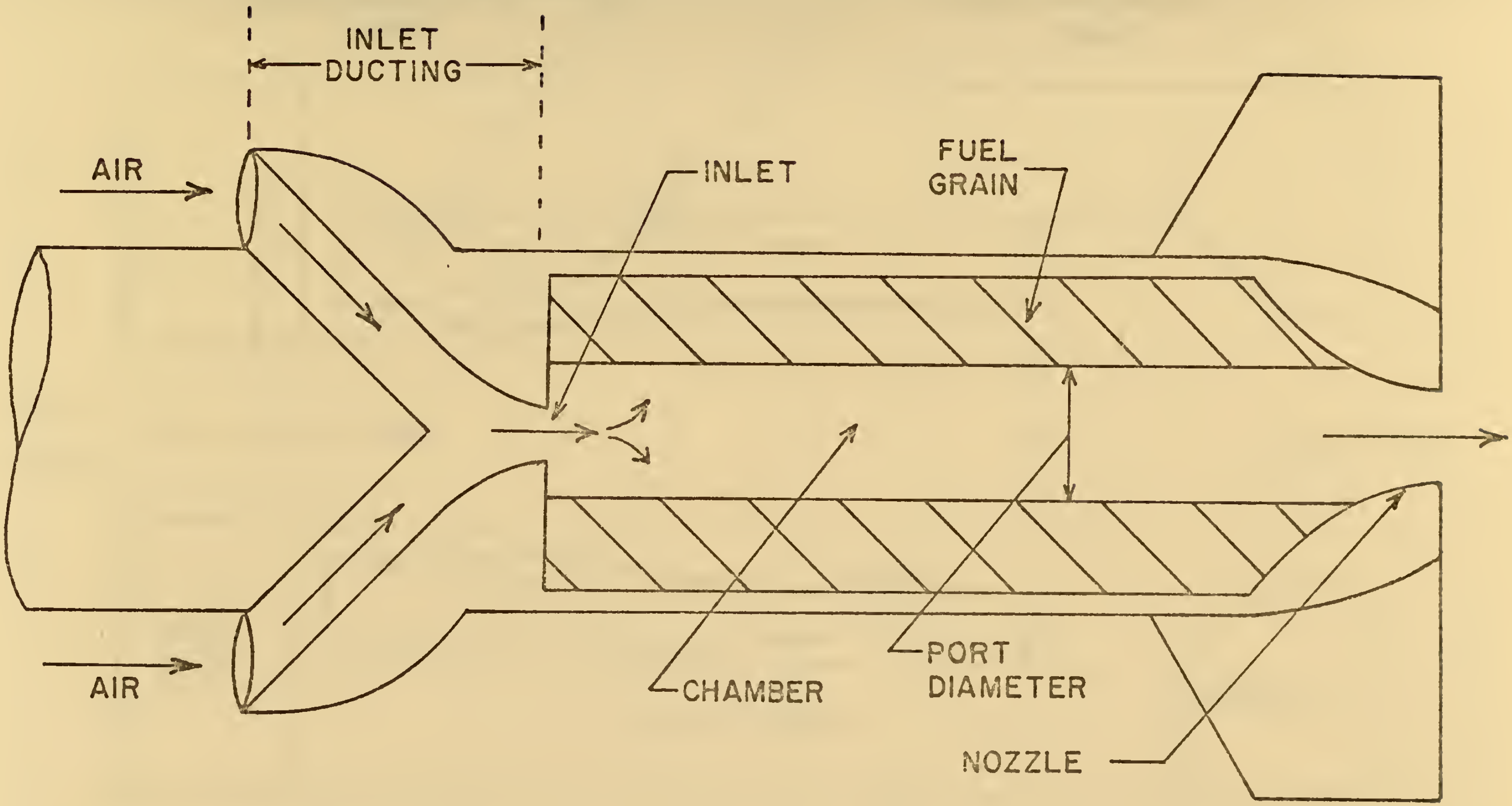

FIGURE 1. POSSIBLE DESIGN OF SOLID FUEL RAMJET COMBUSTOR

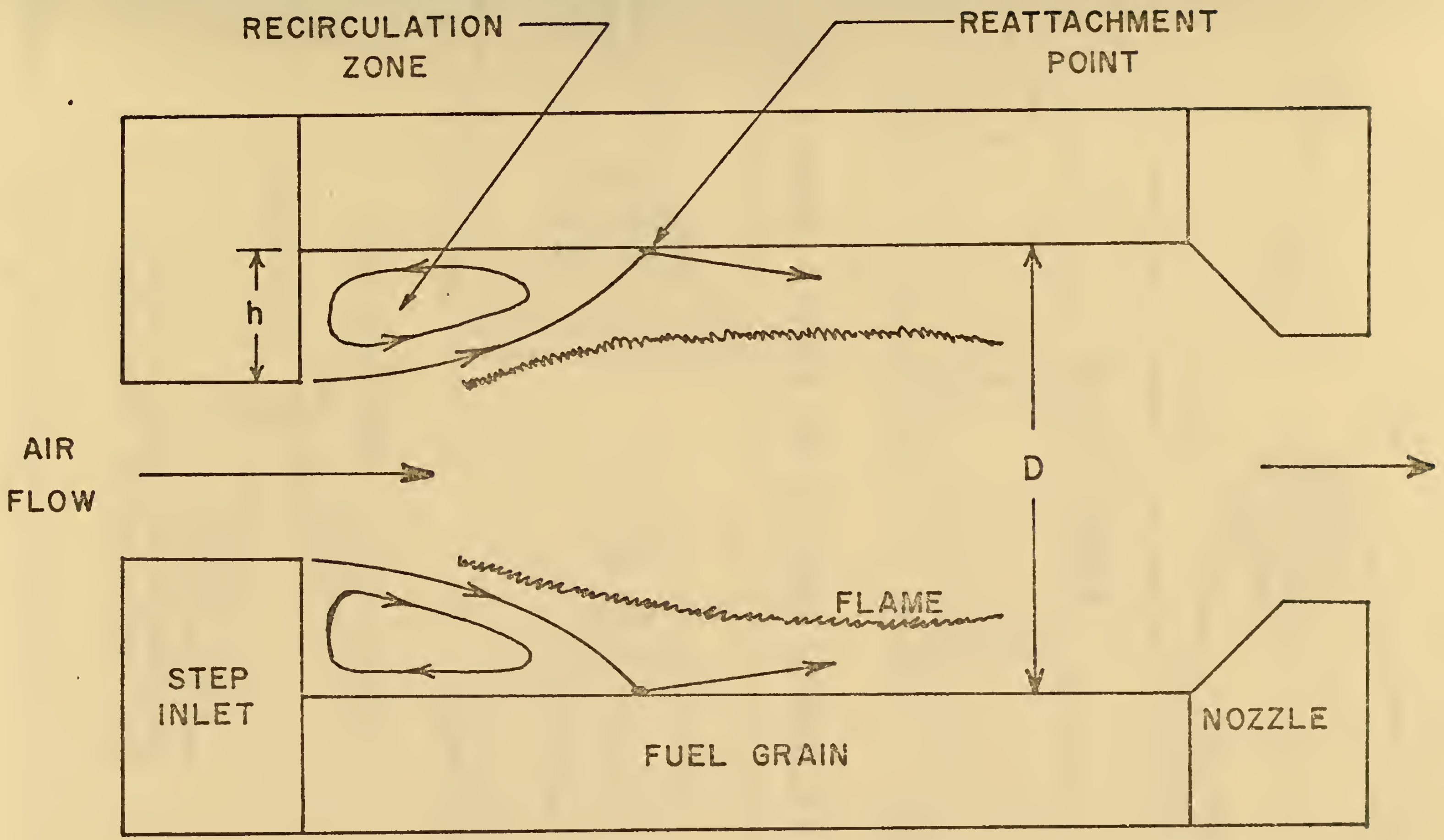

FIGURE 2. INTERNAL BALLISTICS USING REARWARD FACING STEP DESIGN

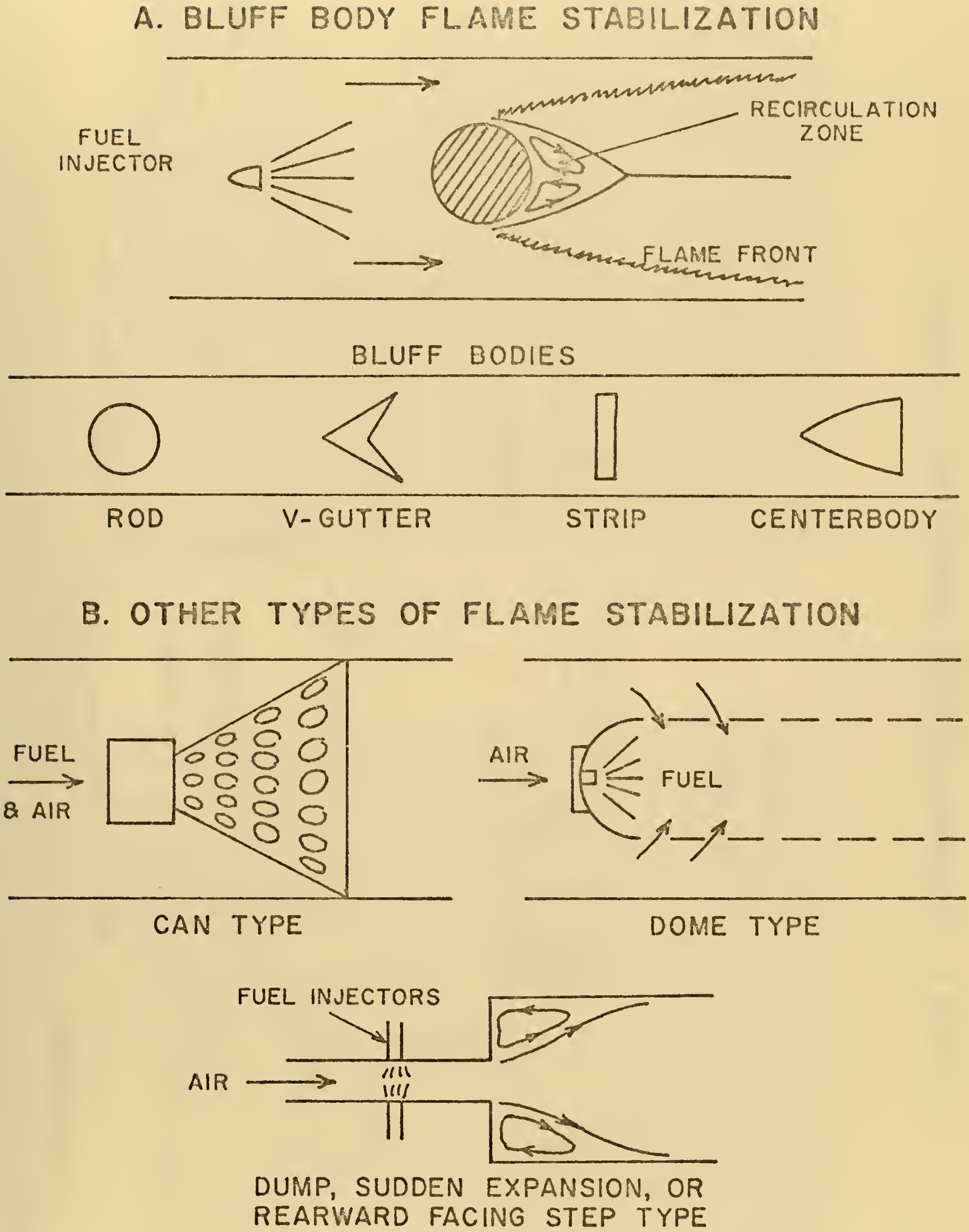

FIGURE 3. FLAME STABILIZATION DEVICES USED IN LIQUID FUEL RAMJETS AND TURBOJETS

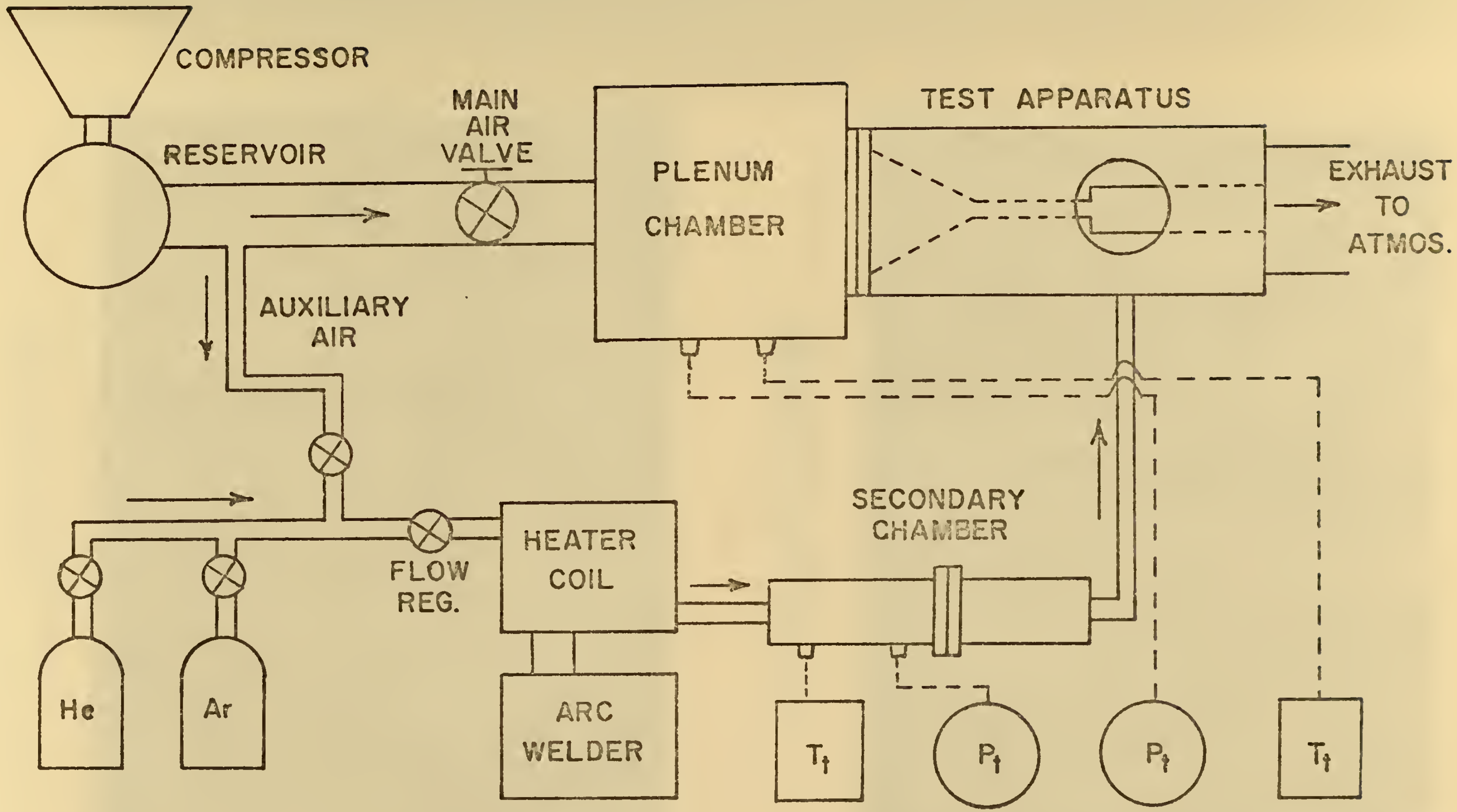

FIGURE 4. SCHEMATIC OF FLOW VISUALIZATION APPARATUS

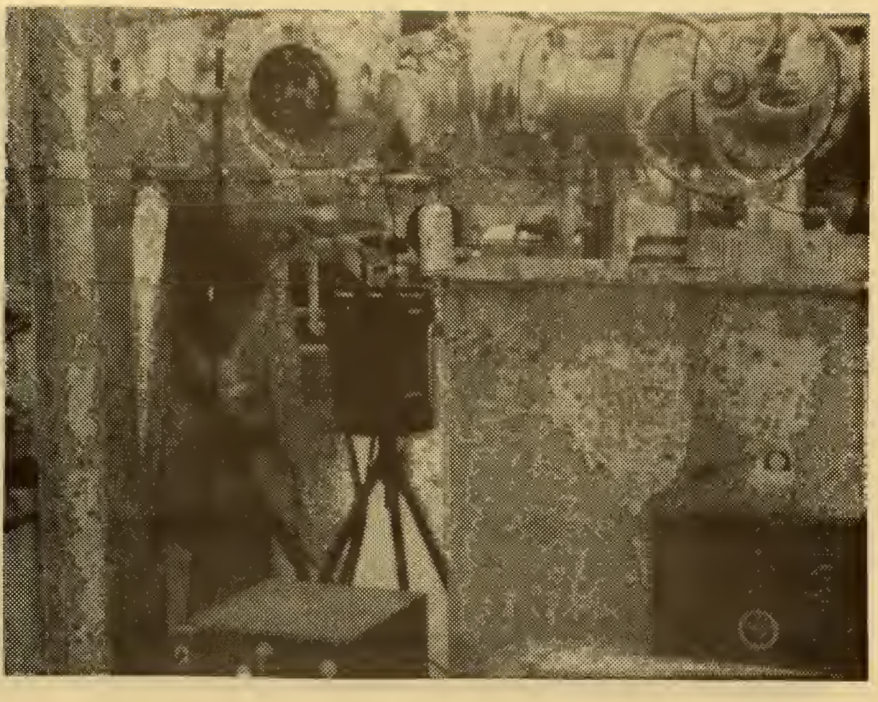

FIGURE 5. NON-REACTING FLOW RIG,
HEATER AND MAIN AIR VALVE

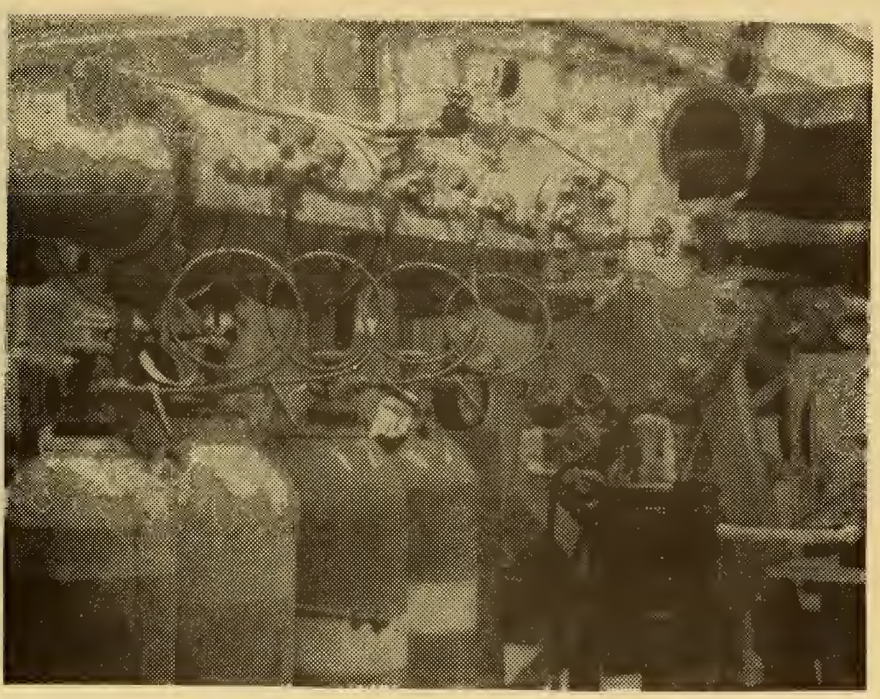

FIGURE 6. NON-REACTING FLOW RIG,
INERT GAS SUPPLY

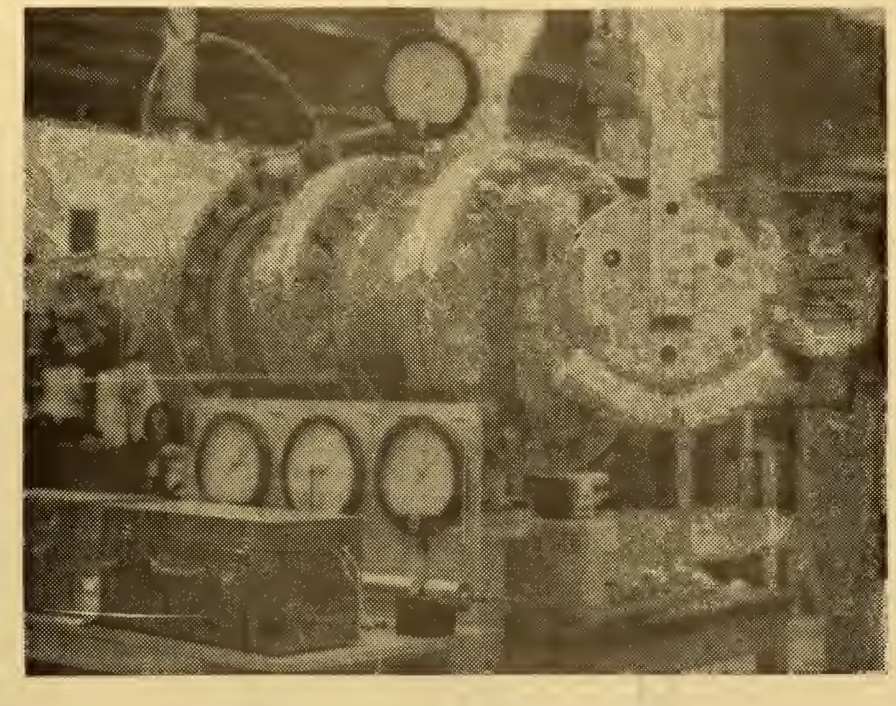

FIGURE 7. NON-REACTING FLOW RIG,
DATA ACQUISITION

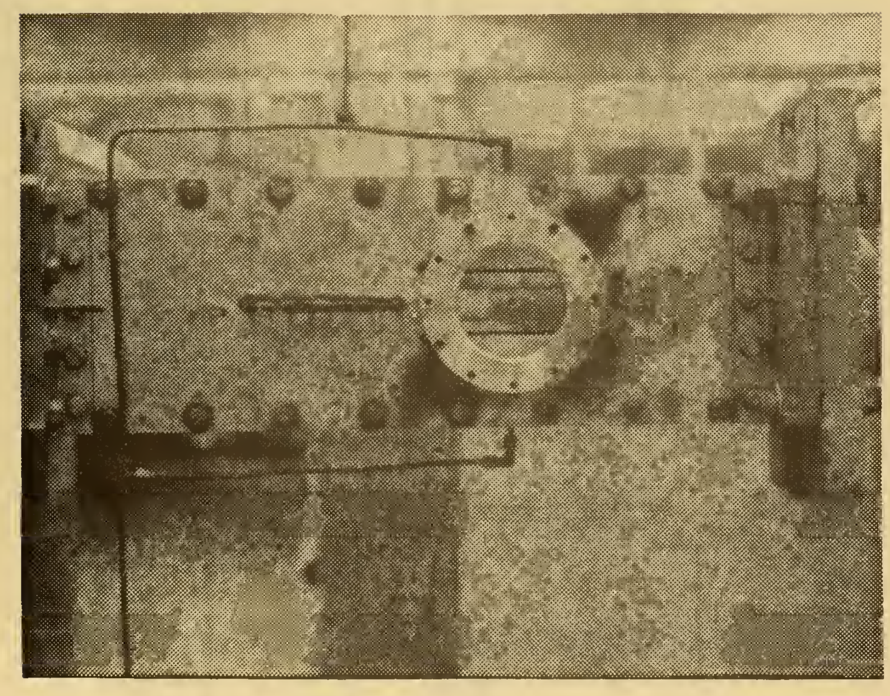

FIGURE 8. NON-REACTING FLOW RIG,
TEST SECTION

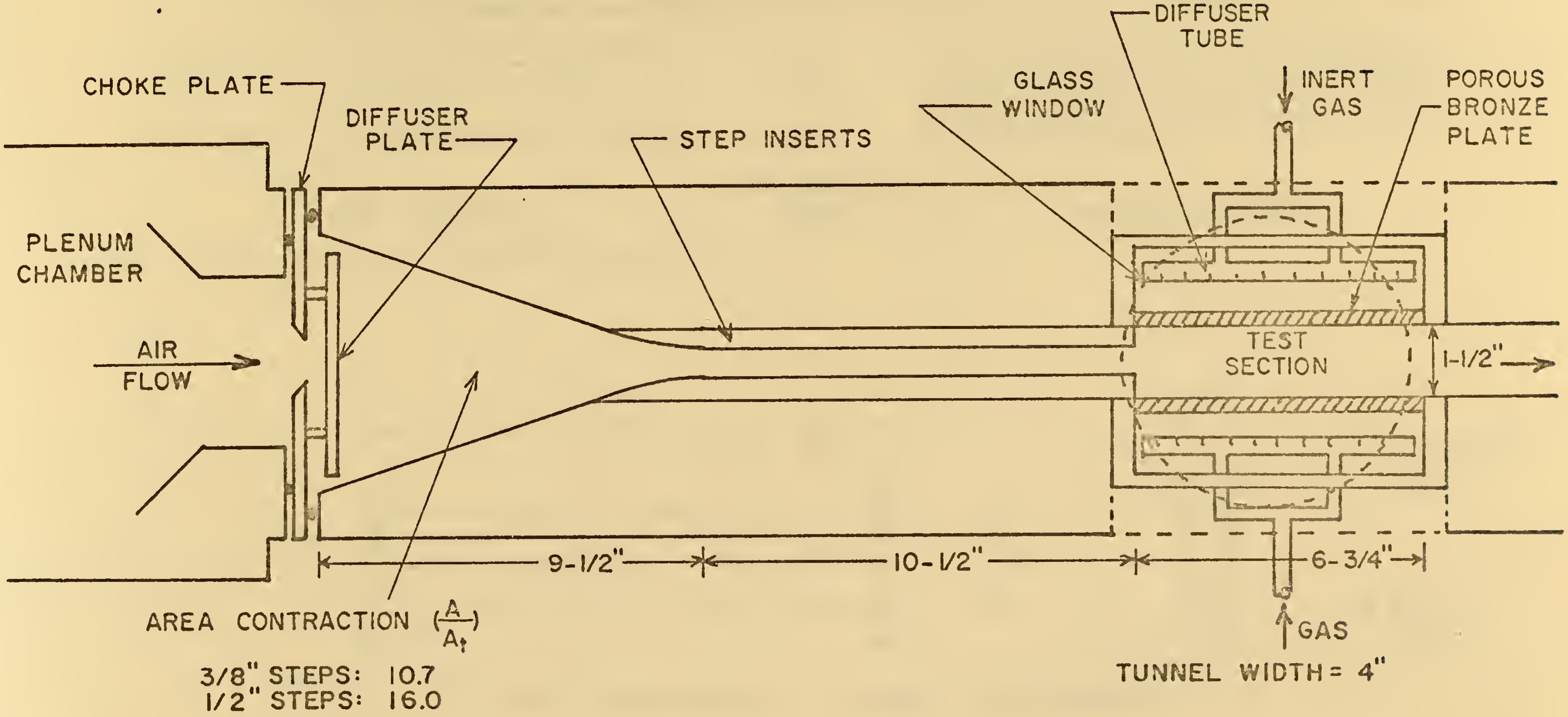

FIGURE 9. TWO-DIMENSIONAL PLANAR FLOW VISUALIZATION APPARATUS

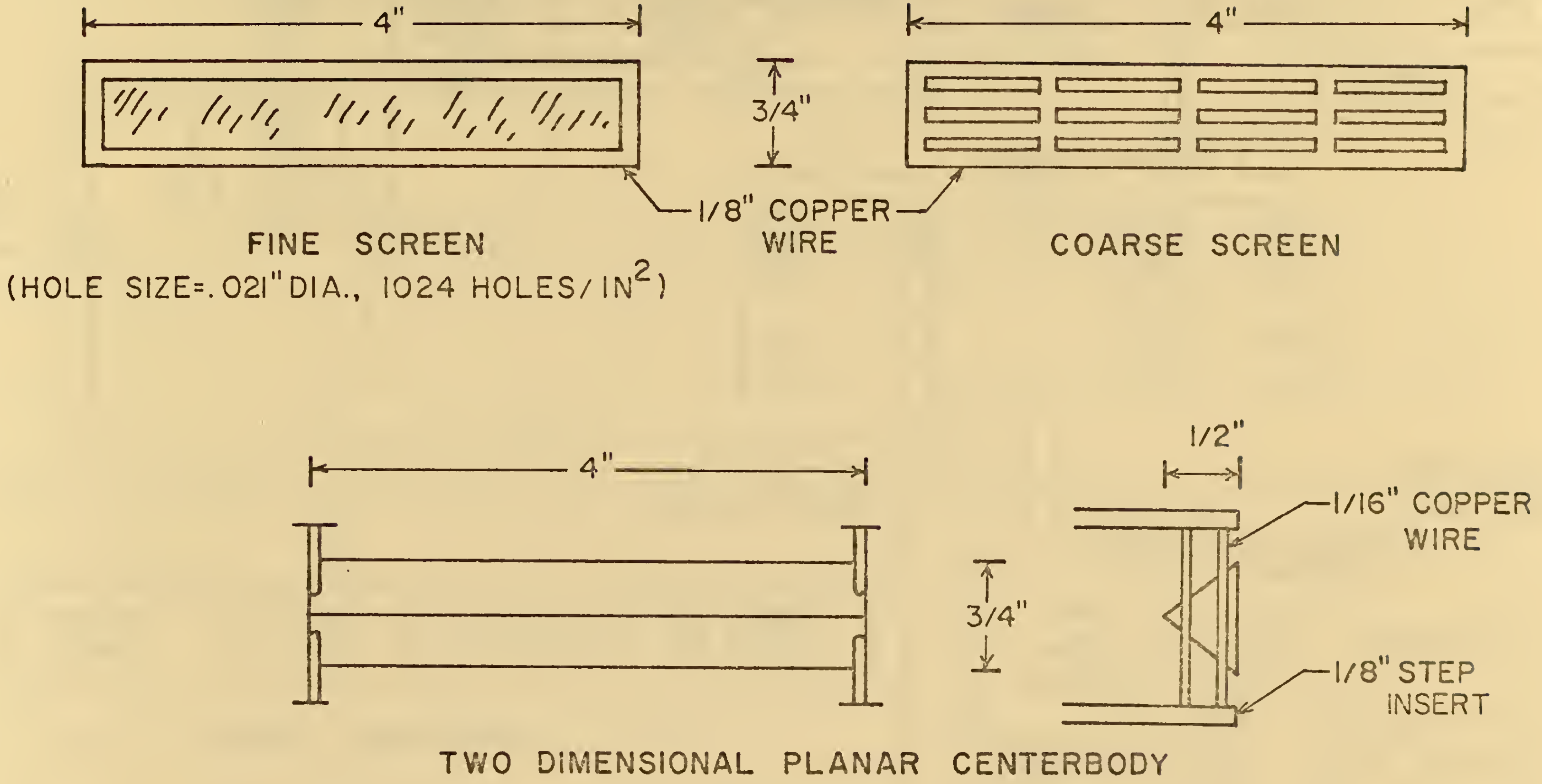

FIGURE 10. PERIPHERAL EQUIPMENT FOR NON-REACTING FLOW TESTS

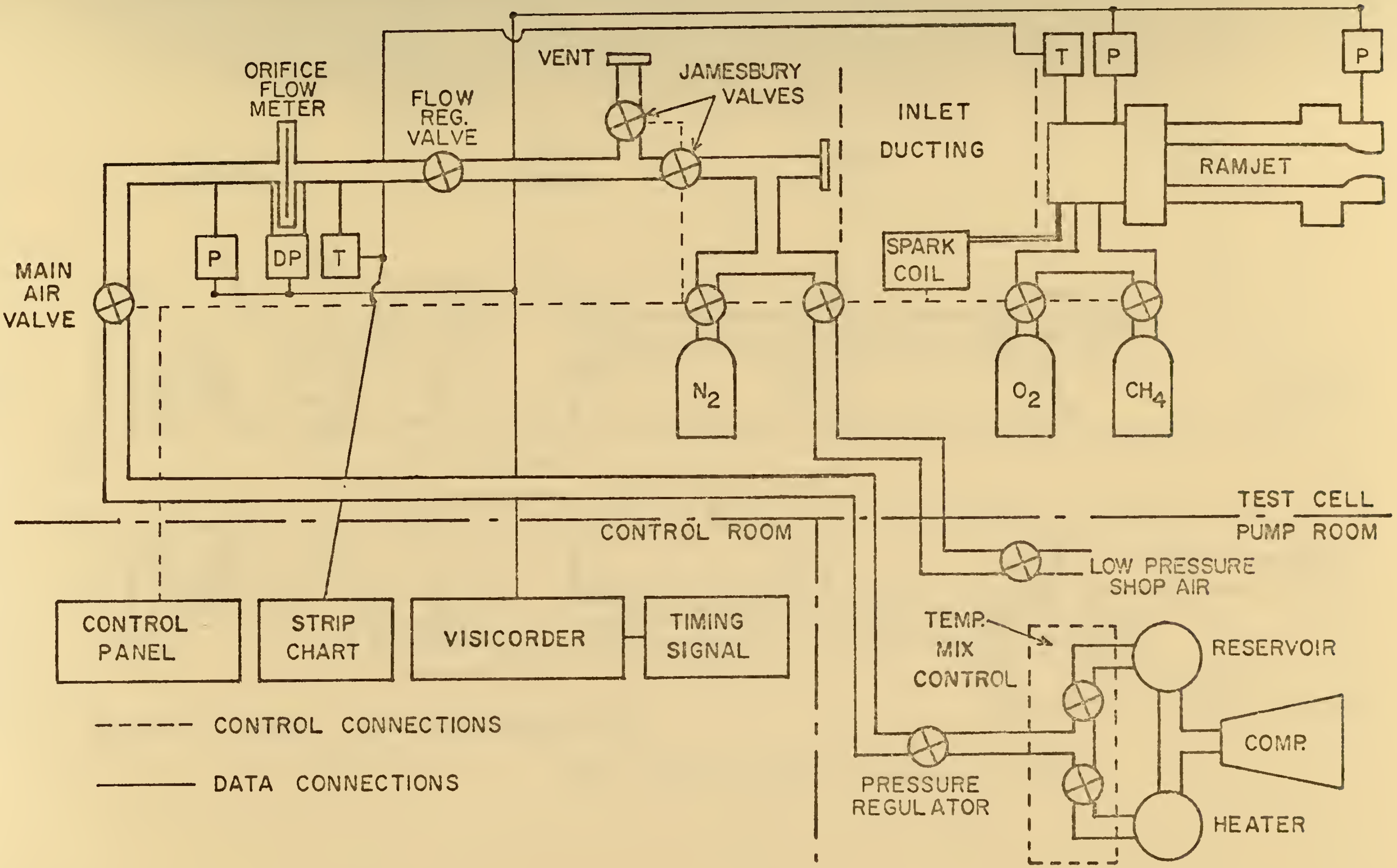

FIGURE 11. SCHEMATIC OF SOLID FUEL RAMJET APPARATUS

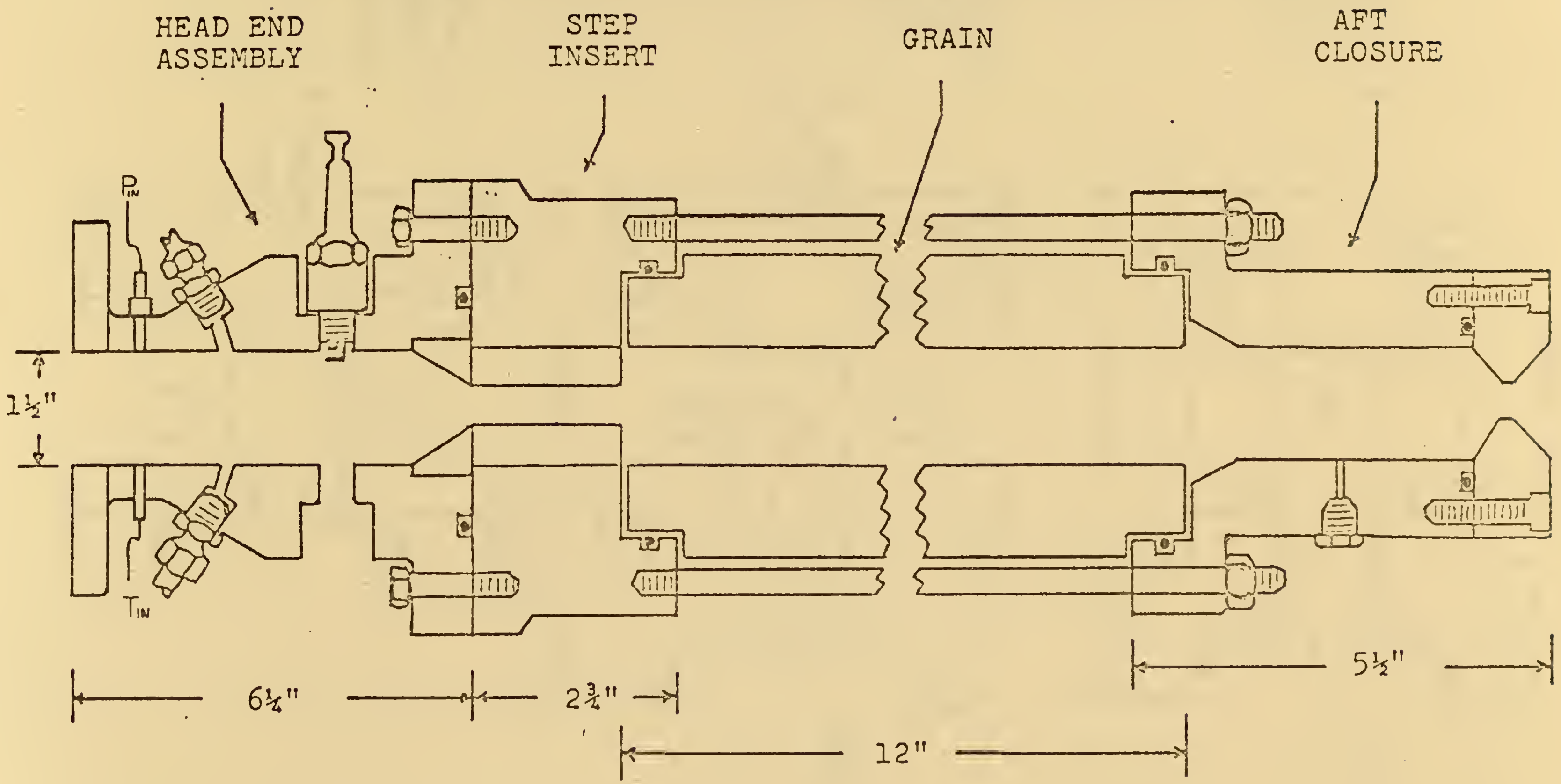

FIGURE 12. SOLID FUEL RAMJET MOTOR
(CONFIGURATION A)

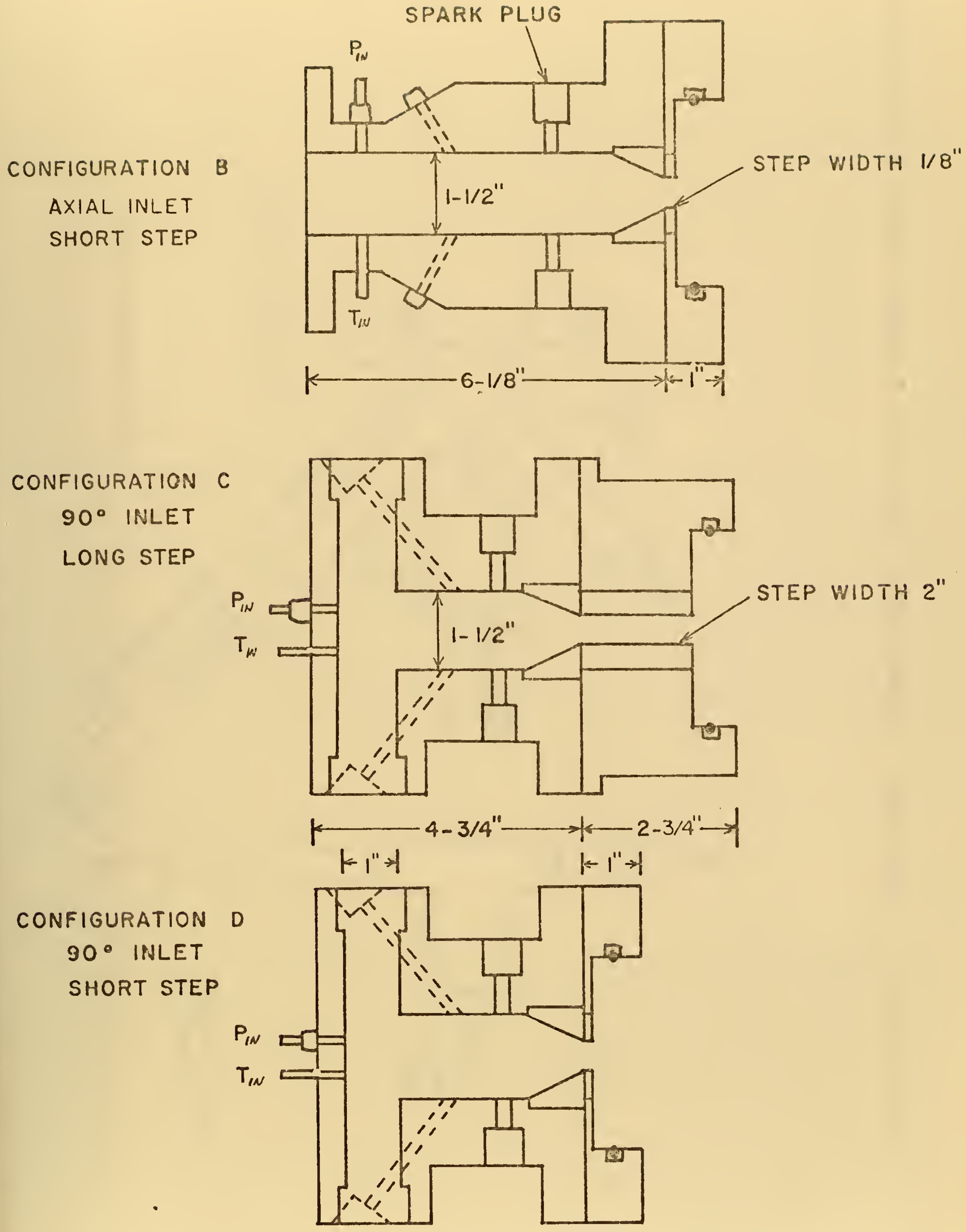

FIGURE 13. MOTOR HEAD CONFIGURATIONS

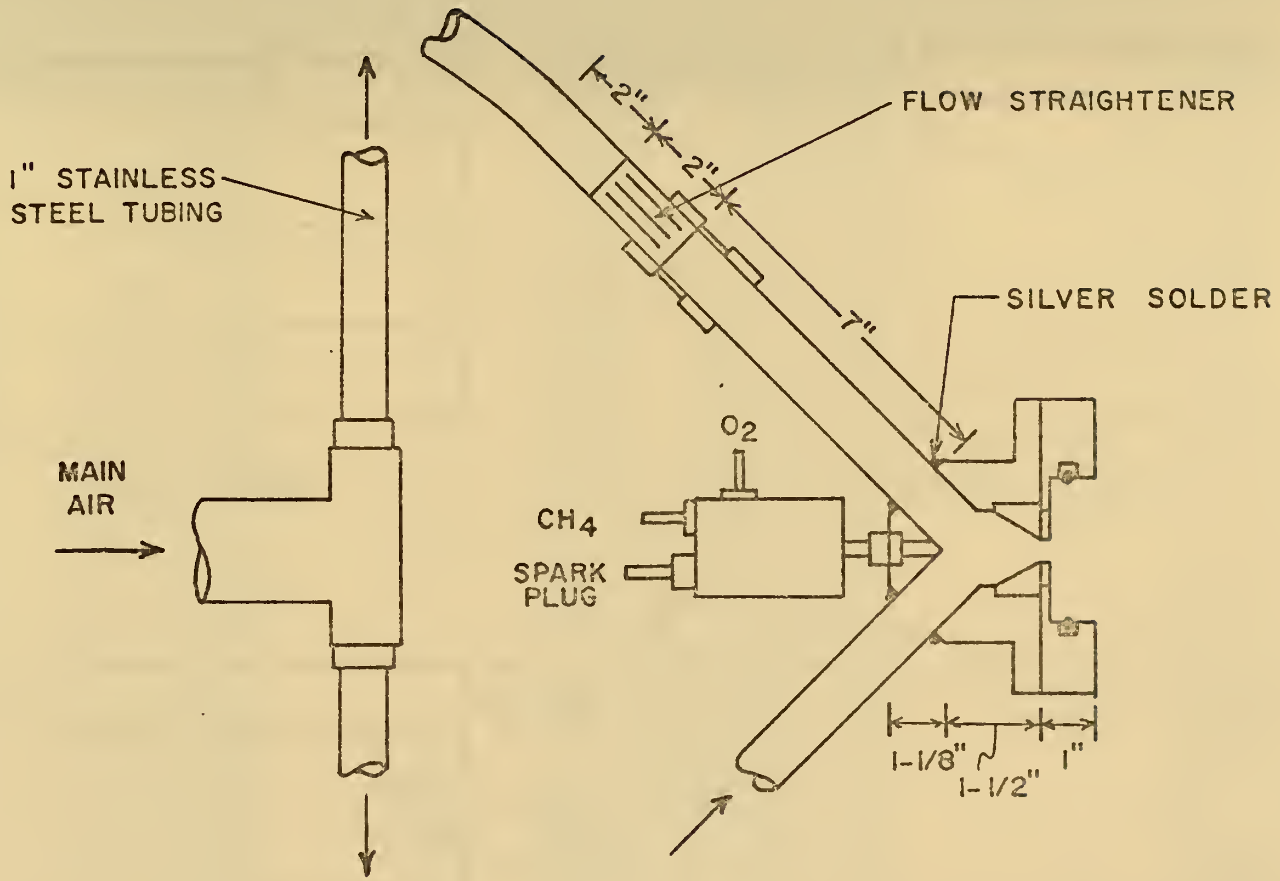

FIGURE 14. CONFIGURATION E (45° INLET, SHORT STEP) WITH INLET DUCTING AND IGNITION SYSTEM

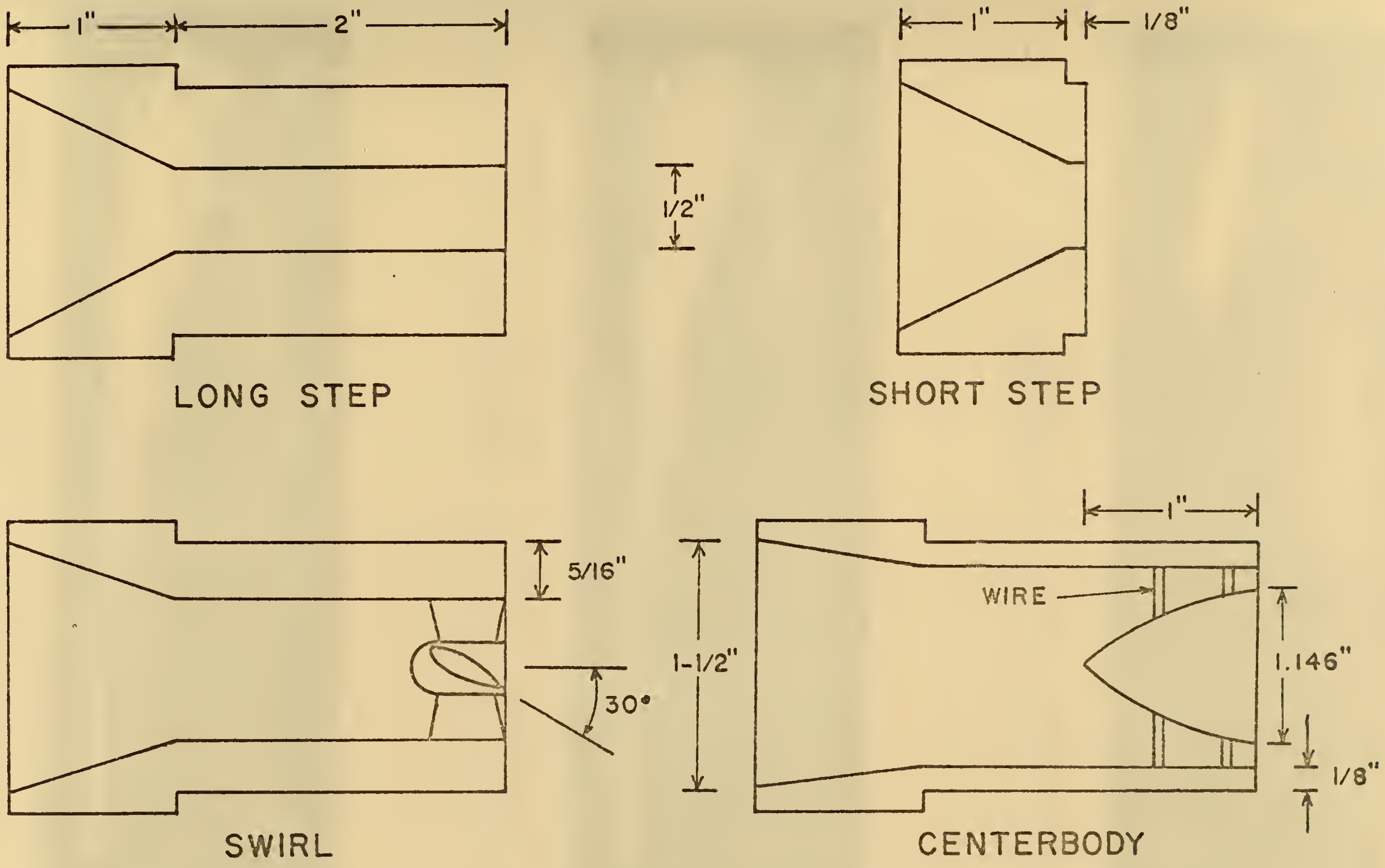

FIGURE 15. AXISYMMETRIC INLET STEP INSERTS

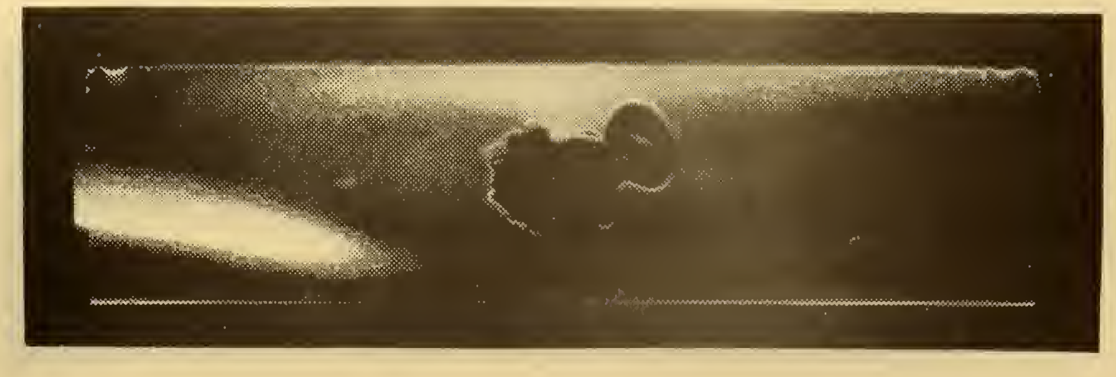

FIGURE 16. LOW INLET ($G = 0.0667$ LBM/SEC-IN^2)
NO BLOWING

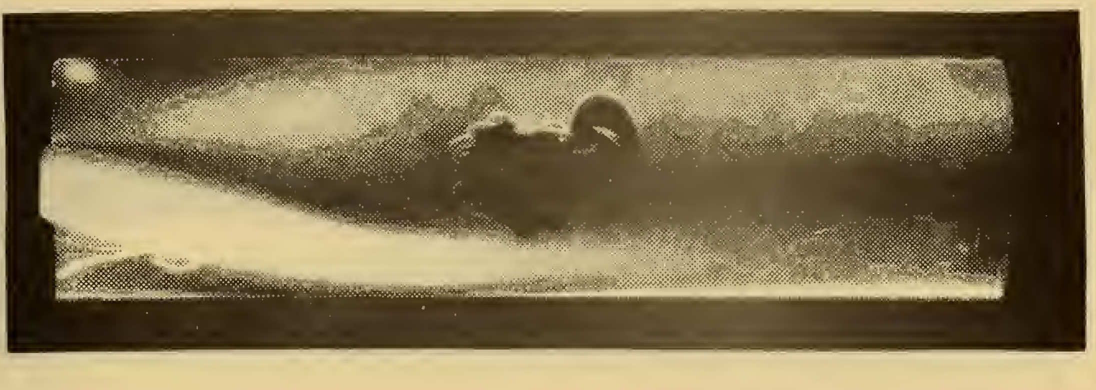

FIGURE 17. HIGH INLET ($G = 0.127$ LBM/SEC-IN^2)
NO BLOWING

FIGURE 18. HIGH INLET ($G = 0.173$ LBM/SEC-IN^2)
NO BLOWING

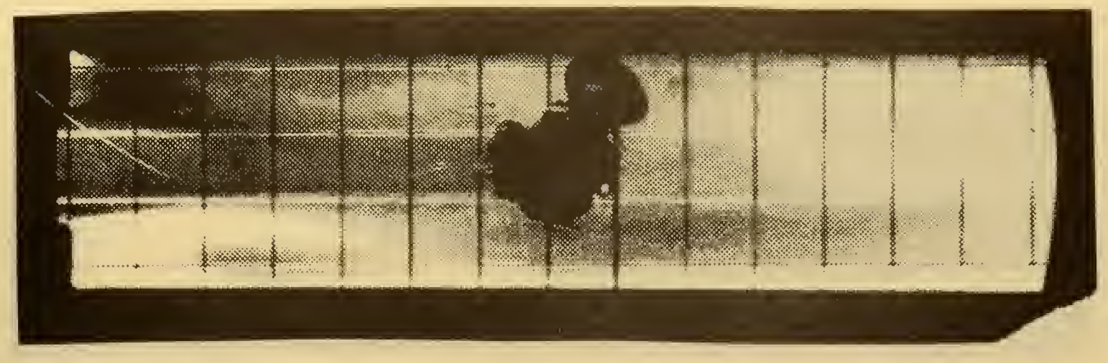

FIGURE 19. <u>3/8" STEP</u>, LOW INLET (G = 0.0779 LBM/SEC-IN^2)
LOW HE BLOWING (G = 0.000149 LBM/SEC-IN^2)

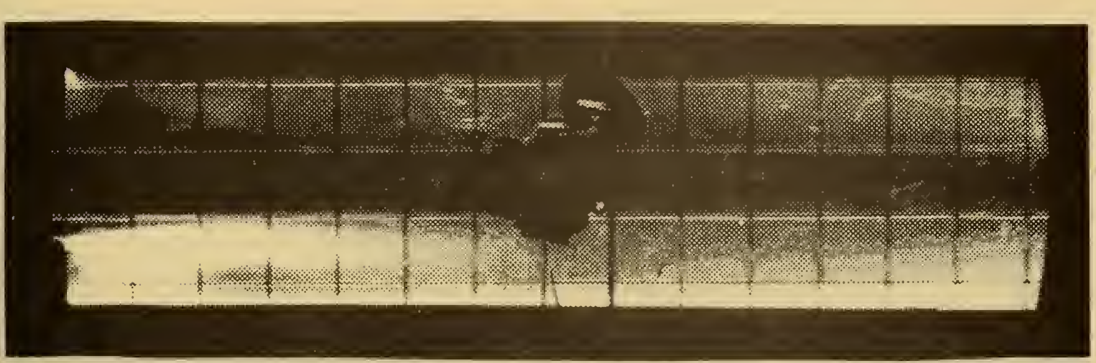

FIGURE 20. <u>3/8" STEP</u>, LOW INLET (G = 0.0750 LBM/SEC-IN^2)
LOW HE BLOWING (G = 0.000277 LBM/SEC-IN^2)

FIGURE 21. LOW INLET (G = 0.0642 LBM/SEC-IN^2)
LOW HE BLOWING (G = 0.000241 LBM/SEC-IN^2)

FIGURE 22. LOW INLET (G = 0.0658 LBM/SEC-IN^2)
LOW HE BLOWING (G = 0.000233 LBM/SEC-IN^2)

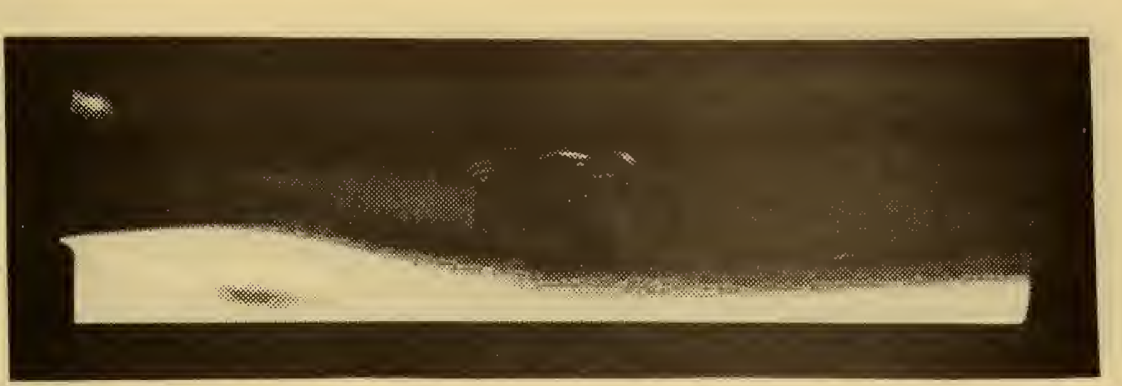

FIGURE 23. LOW INLET (G = 0.0642 LBM/SEC-IN^2)
HIGH HE BLOWING (G = 0.000463 LBM/SEC-IN^2)

FIGURE 24. HIGH INLET (G = 0.124 LBM/SEC-IN^2)
LOW HE BLOWING (G = 0.000239 LBM/SEC-IN^2)

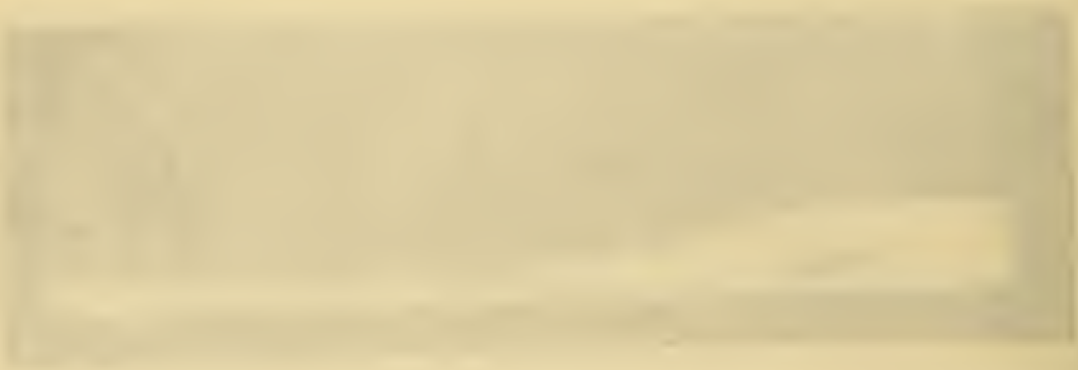

[illegible]

[illegible]

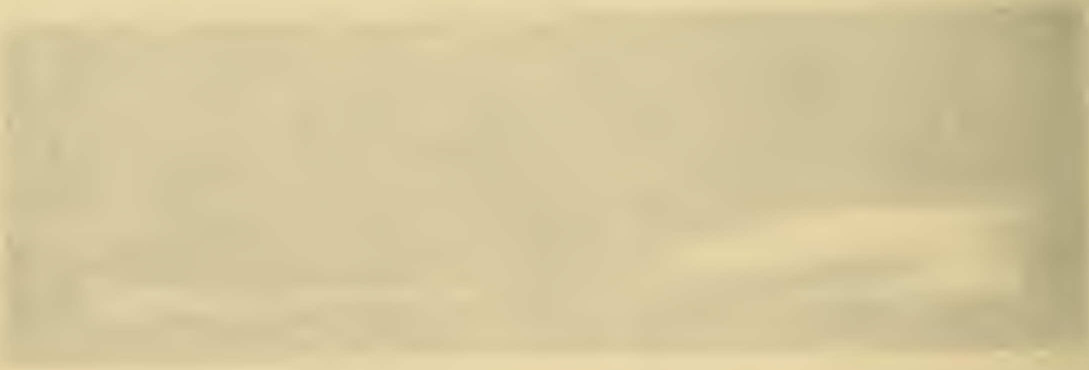

[illegible]

FIGURE 25. HIGH INLET ($G = 0.128$ LBM/SEC-IN^2)
LOW HE BLOWING ($G = 0.000243$ LBM/SEC-IN^2)

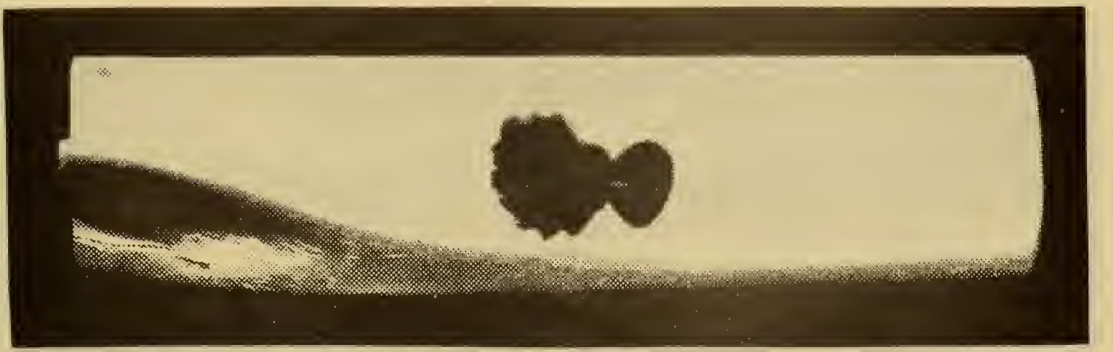

FIGURE 26. HIGH INLET ($G = 0.117$ LBM/SEC-IN^2)
LOW HE BLOWING ($G = 0.000249$ LBM/SEC-IN^2)
(REVERSED KNIFE EDGE)

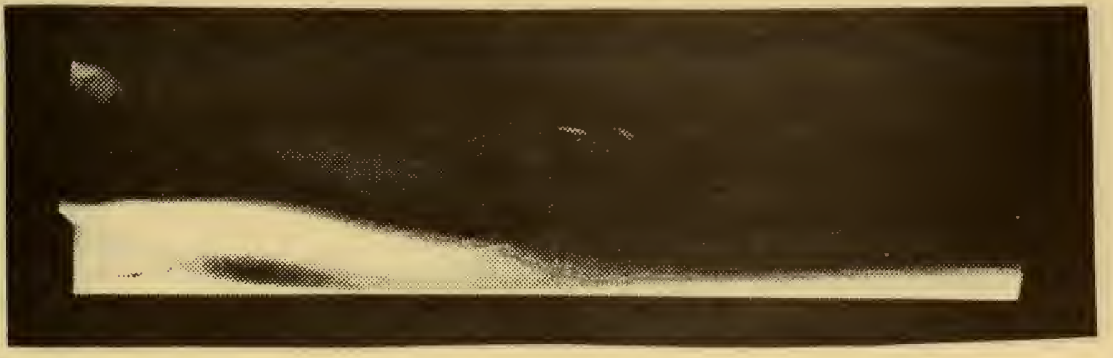

FIGURE 27. HIGH INLET ($G = 0.123$ LBM/SEC-IN^2)
HIGH HE BLOWING ($G = 0.000464$ LBM/SEC-IN^2)

[illegible]

[illegible]

[illegible]

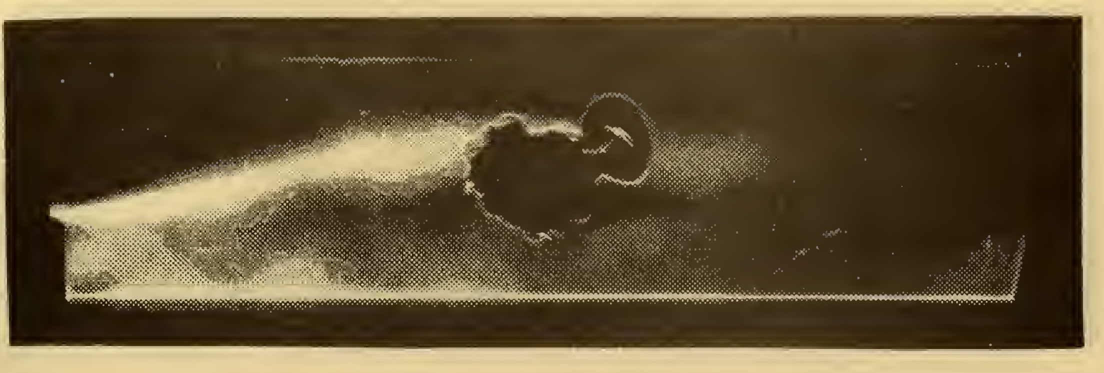

FIGURE 28. LOW INLET ($G = 0.0561$ LBM/SEC-IN^2)
LOW AR BLOWING ($G = 0.000285$ LBM/SEC-IN^2)

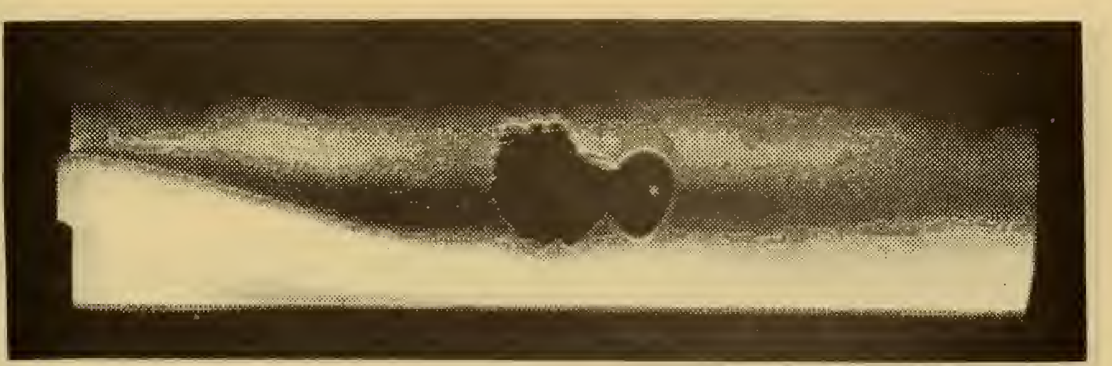

FIGURE 29. LOW INLET ($G = 0.0713$ LBM/SEC-IN^2)
LOW AR BLOWING ($G = 0.000229$ LBM/SEC-IN^2)

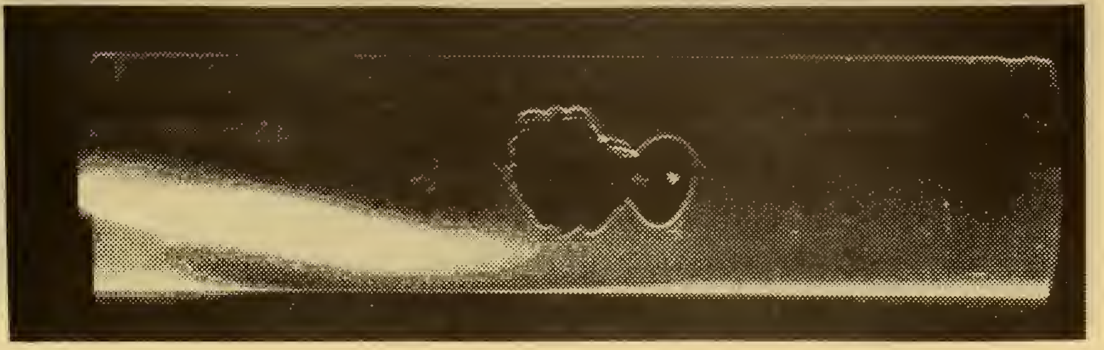

FIGURE 30. MEDIUM INLET ($G= 0.0938$ LBM/SEC-IN^2)
LOW AR BLOWING ($G = 0.000229$ LBM/SEC-IN^2)

FIGURE 31. LOW INLET (G = 0.0832 LBM/SEC-IN^2)
HIGH AR BLOWING (G = 0.000493 LBM/SEC-IN^2)

FIGURE 32. HIGH INLET (G = 0.122 LBM/SEC-IN^2)
LOW AR BLOWING (G = 0.000230 LBM/SEC-IN^2)

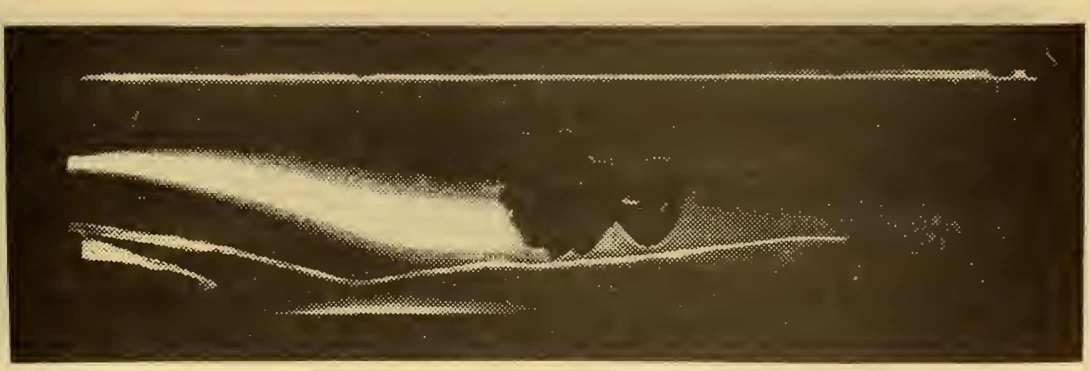

FIGURE 33. HIGH INLET (G = 0.122 LBM/SEC-IN^2)
LOW AR BLOWING (G = 0.000230 LBM/SEC-IN^2)
(REVERSED KNIFE EDGE)

FIGURE 34. HIGH INLET ($G = 0.120$ LBM/SEC-IN^2)
LOW AR BLOWING ($G = 0.000286$ LBM/SEC-IN^2)

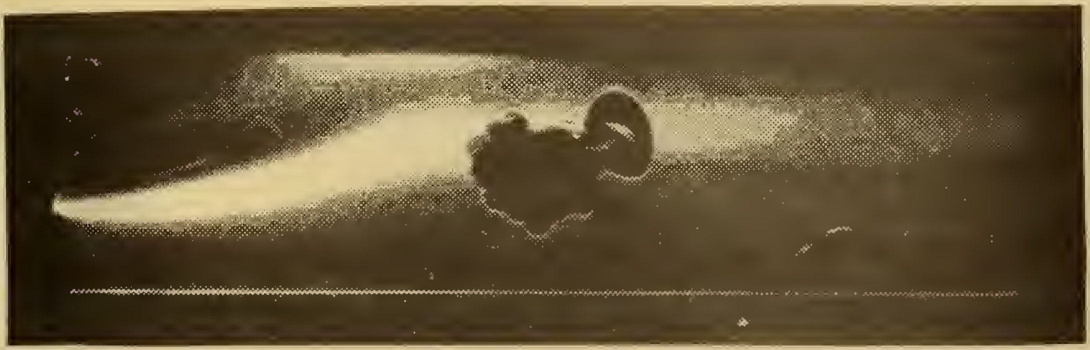

FIGURE 35. HIGH INLET ($G = 0.119$ LBM/SEC-IN^2)
HIGH AR BLOWING ($G = 0.000443$ LBM/SEC-IN^2)

FIGURE 36. LOW INLET ($G = 0.0717$ LBM/SEC-IN^2)
LOW HE BLOWING ($G = 0.000241$ LBM/SEC-IN^2)
(FINE SCREEN)

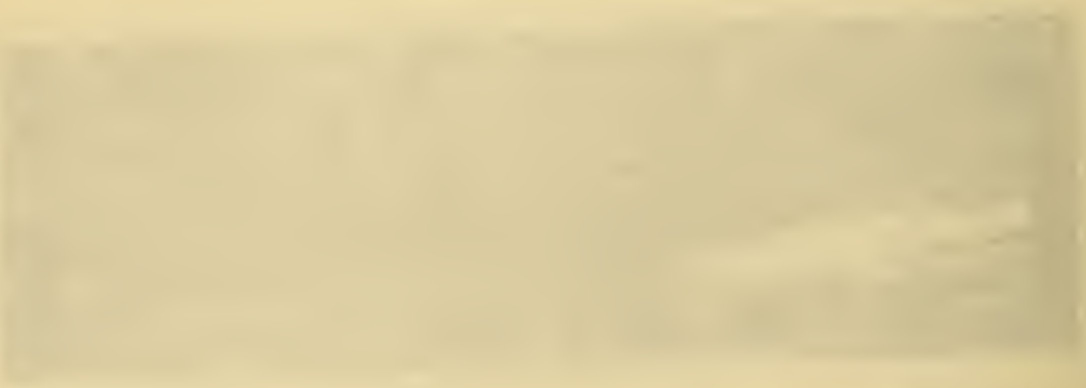

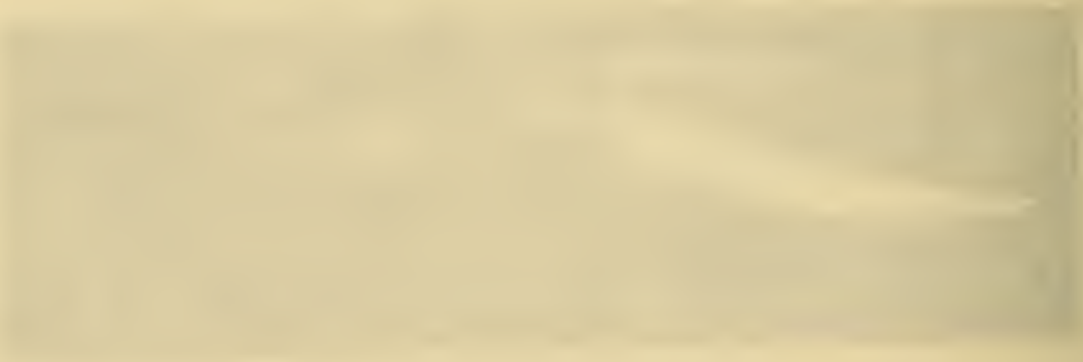

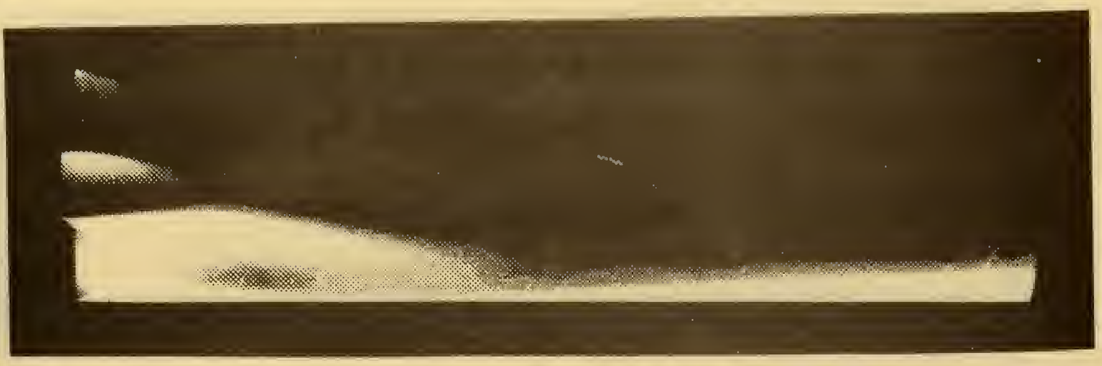

FIGURE 37. MEDIUM INLET ($G = 0.0944$ LBM/SEC-IN^2)
LOW HE BLOWING ($G = 0.000233$ LBM/SEC-IN^2)
(FINE SCREEN)

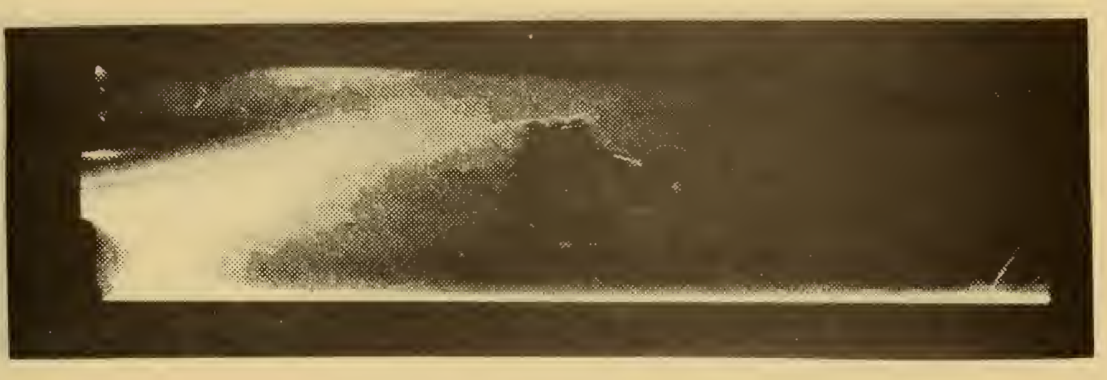

FIGURE 38. HIGH INLET ($G = 0.121$ LBM/SEC-IN^2)
LOE HE BLOWING ($G = 0.000239$ LBM/SEC-IN^2)
(FINE SCREEN)

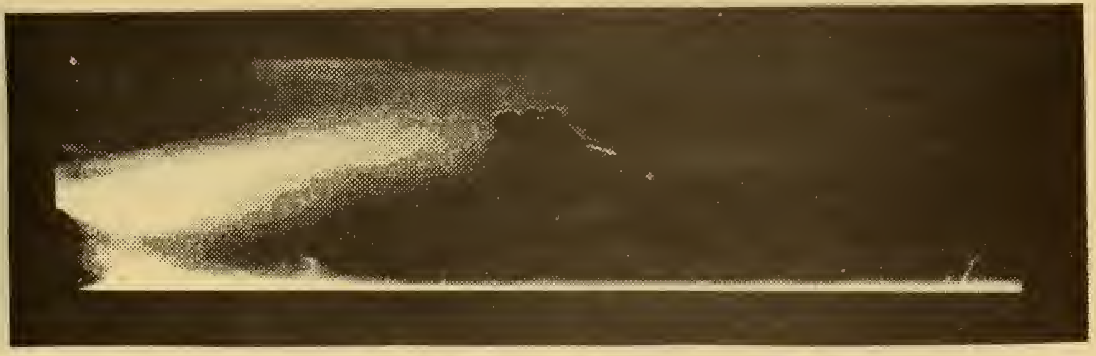

FIGURE 39. HIGH INLET ($G = 0.124$ LBM/SEC-IN^2)
LOW HE BLOWING ($G = 0.000236$ LBM/SEC-IN^2)
(FINE SCREEN)

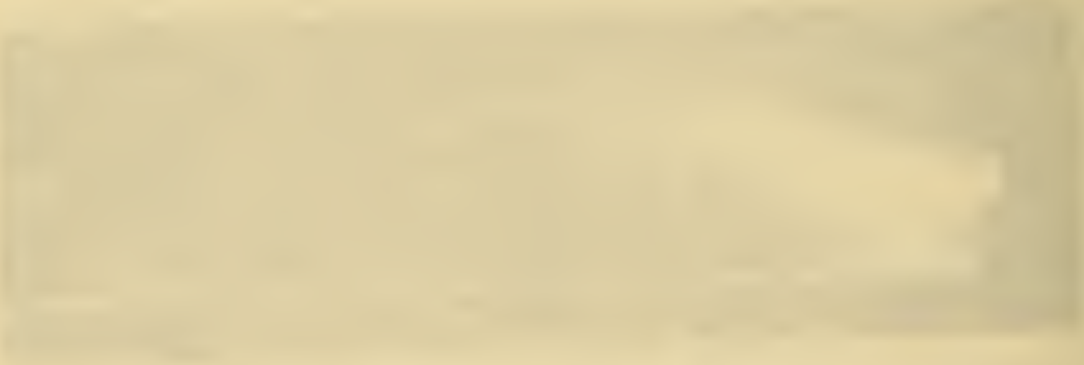

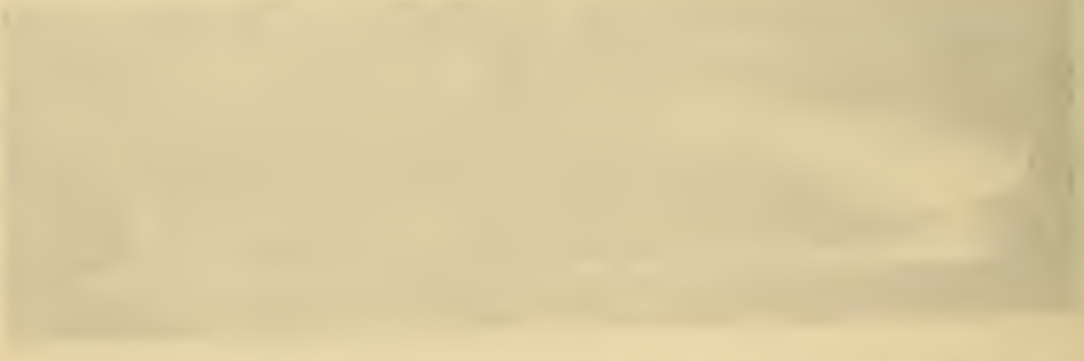

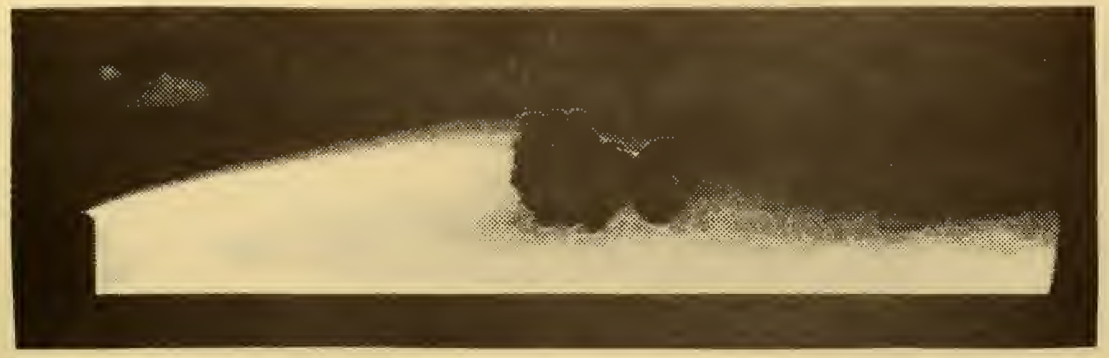

FIGURE 40. LOW INLET ($G = 0.0628$ LBM/SEC-IN^2)
LOW HE BLOWING ($G = 0.000238$ LBM/SEC-IN^2)
(COARSE SCREEN)

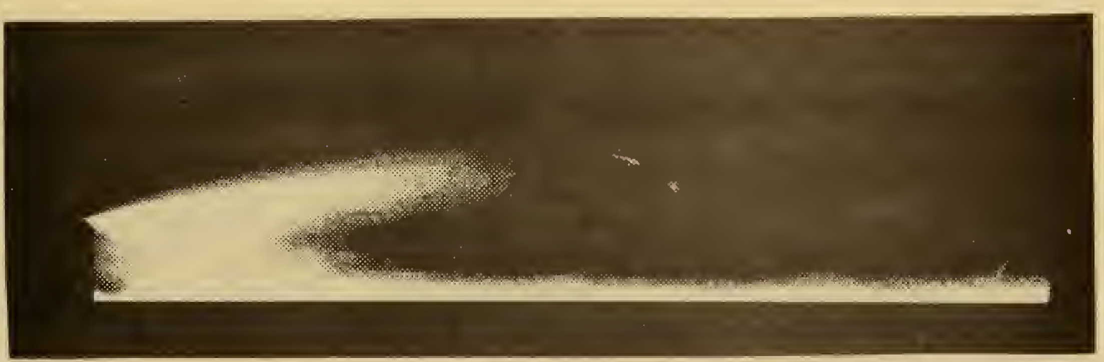

FIGURE 41. LOW INLET ($G = 0.0703$ LBM/SEC-IN^2)
LOW HE BLOWING ($G = 0.000234$ LBM/SEC-IN^2)
(COARSE SCREEN)

FIGURE 42. MEDIUM INLET ($G = 0.0890$ LBM/SEC-IN^2)
LOW HE BLOWING ($G = 0.000247$ LBM/SEC-IN^2)
(COARSE SCREEN)

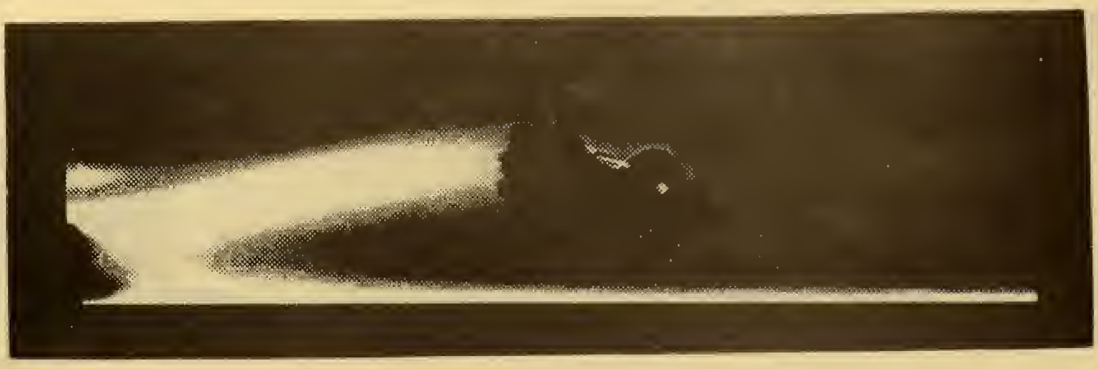

FIGURE 43. HIGH INLET ($G = 0.119$ LBM/SEC-IN^2)
LOW HE BLOWING ($G = 0.000243$ LBM/SEC-IN^2)
(COARSE SCREEN)

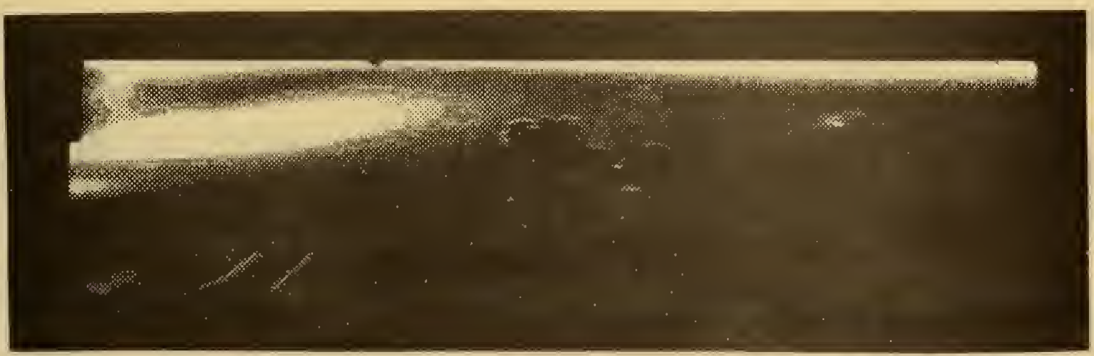

FIGURE 44. HIGH INLET ($G = 0.121$ LBM/SEC-IN^2)
LOW HE BLOWING ($G = 0.000241$ LBM/SEC-IN^2)
(COARSE SCREEN -- REVERSED KNIFE EDGE)

FIGURE 45. HIGH INLET ($G = 0.123$ LBM/SEC-IN^2)
HIGH HE BLOWING ($G = 0.000410$ LBM/SEC-IN^2)
(COARSE SCREEN)

FIGURE 46. LOW INLET ($G = 0.066$ LBM/SEC-IN^2)
NO BLOWING
CENTERBODY

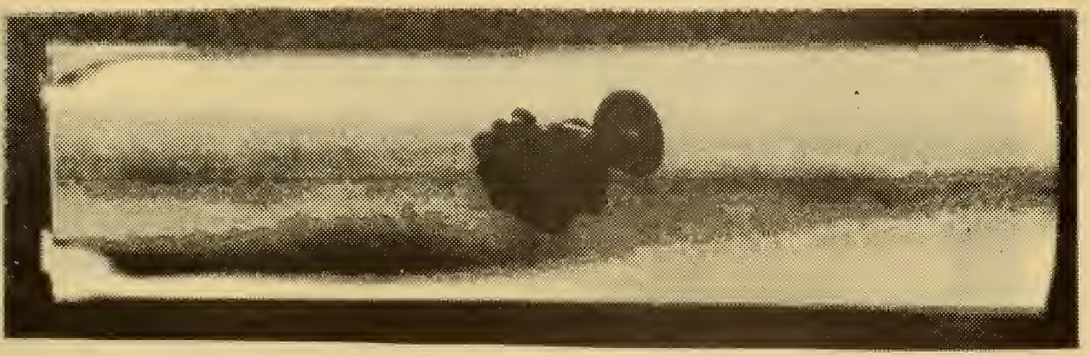

FIGURE 47. HIGH INLET ($G = 0.117$ LBM/SEC-IN^2)
NO BLOWING
CENTERBODY

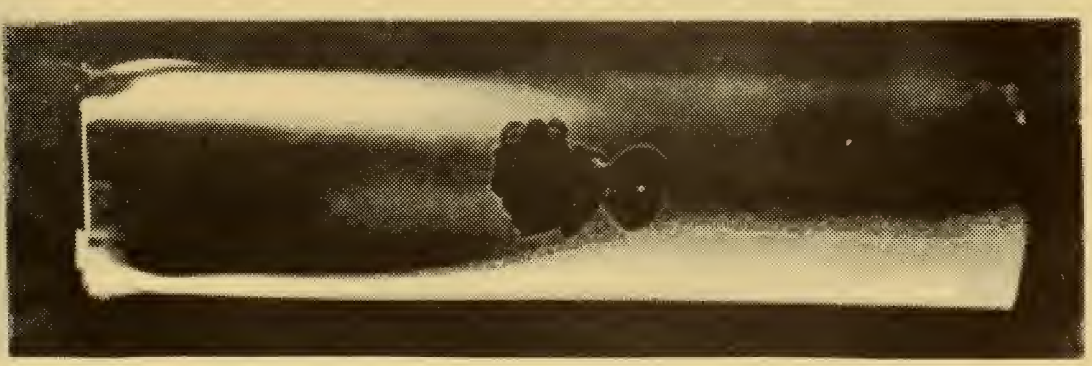

FIGURE 48. LOW INLET ($G = 0.075$ LBM/SEC-IN^2)
LOW HE BLOWING ($G = 0.000237$ LBM/SEC-IN^2)
CENTERBODY

FIGURE 49. LOW INLET (G = 0.073 LBM/SEC-IN^2)
LOW HE BLOWING -- UNHEATED (G = 0.000261-
CENTERBODY LBM/SEC-IN^2)

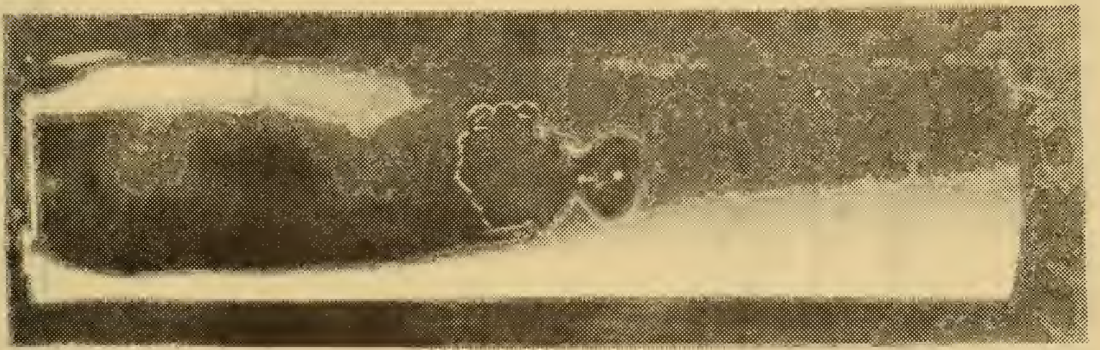

FIGURE 50. HIGH INLET (G = 0.116 LBM/SEC-IN^2)
LOW HE BLOWING (G = 0.000238 LBM/SEC-IN^2)
CENTERBODY

FIGURE 51. HIGH INLET (G = 0.127 LBM/SEC-IN^2)
HIGH HE BLOWING (G = 0.000405 LBM/SEC-IN^2)
CENTERBODY

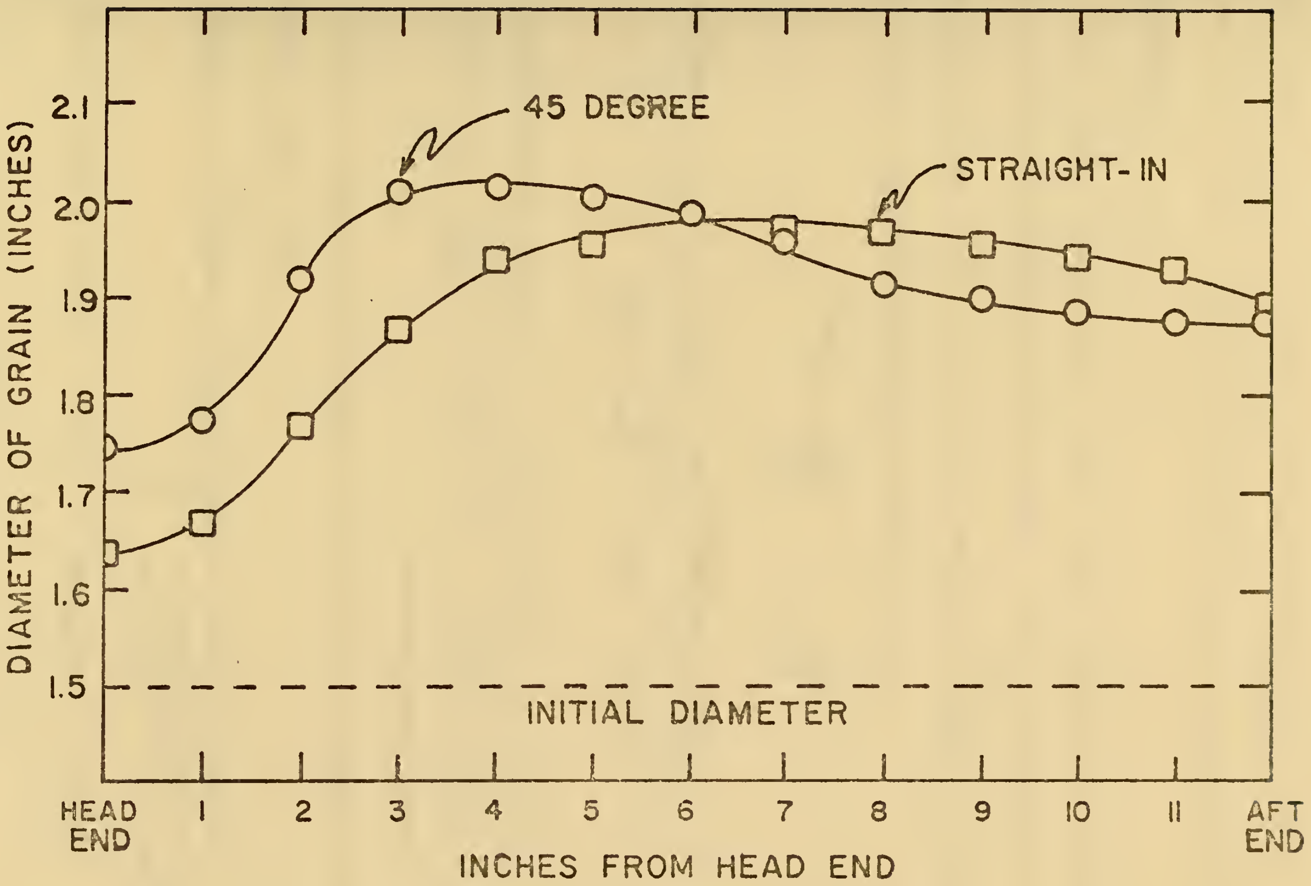

FIGURE 52. COMPARISON OF REGRESSION RATES OBTAINED WITH 45 DEGREE AND STRAIGHT-IN INLET DUCTING

APPENDIX A: SIMILARITY BETWEEN NON-REACTING AND REACTING TEST DATA

Non-reacting tests were performed with a two-dimensional, planar test section. To achieve similarity with inlet mass flow rates and regression rates achieved by Boaz in reacting tests, identical Reynolds numbers were considered to be most important.

A. For inlet conditions, $Re_D = Re_D'$ where both Reynolds numbers are based upon port diameter. Re_D = Reynolds number in reacting flow tests with a cylindrical grain, Re_D' = Reynolds number for two-dimensional planar flow.

$$Re_D = \frac{\rho V D}{\mu} = \frac{\dot{m} D}{\mu A}$$

Since $D = D'$, $\mu = \mu'$, then for $Re_D = Re_D'$

$$\frac{\dot{m}}{A} = \frac{\dot{m}'}{A'} \quad \text{or} \quad G = G'$$

From Boaz's data: $0.10 < \dot{m}_{air} < 0.22$ lbm/sec

Since $A = \frac{\pi D^2}{4} = 1.7671 \text{ in}^2$, $\underline{0.0566 < G_{air} < 0.124}$ lbm/sec-in^2

B. For wall mass addition, similarity is again achieved by matching mass flux.

$\dot{m}_{fuel} = \dot{r} A \rho_{PMM}$ where ρ_{PMM} = 0.0433 lbm/in^3
$\dot{r}$ = regression rate
A = intersurface area

From Boaz's data: $0.01 < \dot{m}_{fuel} < 0.036$ lbm/sec

Since $A = \pi D L = 56.549 \text{ in}^2$, $\underline{0.000177 < G_{fuel} < 0.000637}$ lbm/sec-in^2

APPENDIX B: BLOW-OFF LIMIT DATA

A. AXIAL DUCTING WITH FLOW STRAIGHTENERS (UNLESS OTHERWISE STATED)

Configuration	Lowest G Tested LBM/SEC-IN^2	Highest G Tested LBM/SEC-IN^2	Remarks
"A", 1/2" step	0.138	0.160	Sustained Combustion
"B", 1/2" step	0.081	0.162	Sustained Combustion
"B", 1/2" step, no flow straighteners	0.079	0.102	Sustained Combustion
"B", 1/2" step, no flow straighteners	0.103	0.121	Ignition Blow-Out
"A", swirl with 5/16" step	0.055	0.082	No Combustion
"A", centerbody	0.046	0.087*	No Combustion
"A", centerbody	0.085*	0.153	Ignition Blow-Out

---

*Sustained combustion at G = 0.087 lbm/sec-in^2 due to separation of three struts. Replaced struts and got ignition blow-out at G = 0.085 lbm/sec-in^2.

B. 90-DEGREE INLET DUCTING (PIPING WITH NO FLOW STRAIGHTENERS)

Configuration	Lowest G Tested LBM/SEC-IN^2	Highest G Tested LBM/SEC-IN^2	Remarks
"C", 1/2" step	0.083	0.126	No Combustion
"D", 1/2" step	0.085#	0.115	No Combustion

#Sustained combustion at G = 0.085 lbm/sec-in^2 using old grain. Was not repeatable and, therefore, discounted.

C. 45-DEGREE INLET DUCTING (TUBING AND FLOW STRAIGHTENERS)

Configuration	Lowest G Tested LBM/SEC-IN^2	Highest G tested LBM/SEC-IN^2	
"E", 1/2" step	0.085	0.162	Sustained Combustion
"E", 1/2" step, one side closed off	0.083	0.108	No Combustion

APPENDIX C: 30-SECOND HOT FIRING DATA

CONFIGURATION	GAIR LBM/SEC-IN^2	CHAMBER P (PSIA)	RUN TIME SEC	INLET T F	RWT IN/SEC	RDOT IN/SEC	% ERROR
"A", 1/2" step	0.114	59	30.5	65	0.0063	0.00635	.86
"E", 1/2" step	0.119	62	30.6	65	0.0068	0.00663	2.5
"E", 1/2" step	0.111	58	31.0	62	0.0065	0.00622	4.3

where:

1) $$RWT = \frac{\sqrt{\frac{4\,(W_i - W_f)}{\pi \rho L} + d_i^2} - d_i}{2\,\Delta t}$$

W_i = Initial weight of grain

W_f = final weight of grain

ρ = density of fuel

L = grain length

d_i = initial exit diameter of port

2) RDOT = Average regression rate found by Boaz

$$RDOT = C\;P^{0.51}\;T^{0.34}\;G_o^{0.41} \quad \text{(in/sec)}$$

for h/D = 0.333

C = 2.3×10^{-4}

P = chamber pressure (psia)

T = inlet temperature (^{o}R)

G_o = mass flux of air (lbm/sec-in^2)

3) $$\%\ ERROR = \frac{R\,W\,T - RDOT}{RDOT} \times 100$$

LIST OF REFERENCES

1. Netzer, D.W., Hybrid Rocket Internal Ballistics, Naval Postgraduate School, CPIA Publication No. 222, January 1972.

2. Holzman, A.L., Dunlap, R., and Iwanciow, B.L., "Combustion Stabilization in a Solid Fuel Ramjet", Paper presented at the Tenth JANNAF Combustion Meeting, Naval War College, Newport, Rhode Island, August 1973.

3. Gosman, A.D., Pun, W.M., Runchal, A.K., Spalding, D.B., and Wolfshtien, M., Heat and Mass Transfer in Recirculation Flows, Academic Press, 1969.

4. Spalding, D.B., Gosman, A.D., and Pun, W.M., The Prediction of Two-Dimensional Flows, Short Course, Pennsylvania State University, August 1972.

5. Boaz, L.D., Internal Ballistics of Solid Fuel Ramjets, Thesis, Naval Postgraduate School, March 1973.

6. Longwell, J.P., "Combustion Problems in Ramjets", Fifth Symposium (International) on Combustion, Combustion in Engines and Combustion Kinetics, Reinhold Publishing Corp., New York, 1955.

7. Lewis, B. and Von Elbe, G., Combustion, Flames and Explosions of Gases, Second Edition, Academic Press, 1961.

8. Abbott, D.E. and Kline, J.S., "Experimental Investigation of Subsonic Turbulent Flow Over Single and Double Backward Facing Steps", Journal of Basic Engineering, September 1962.

INITIAL DISTRIBUTION LIST

		No. Copies
1.	Defense Documentation Center Cameron Station Alexandria, Virginia 22314	2
2.	Library, Code 0212 Naval Postgraduate School Monterey, California 93940	2
3.	Chairman, Department of Aeronautics Naval Postgraduate School Monterey, California 93940	1
4.	Assoc. Professor D. W. Netzer, Code 57Nt Department of Aeronautics Naval Postgraduate School Monterey, California 93940	2
5.	Lt. C. E. Jones, III, USN Department of Aeronautics Naval Postgraduate School Monterey, California 93940	2
6.	Lt. Lowell D. Boaz, USN Department of Aeronautics Naval Postgraduate School Monterey, California 93940	1

REPORT DOCUMENTATION PAGE		READ INSTRUCTIONS BEFORE COMPLETING FORM
1. REPORT NUMBER	2. GOVT ACCESSION NO.	3. RECIPIENT'S CATALOG NUMBER
4. TITLE (and Subtitle) INVESTIGATIONS INTO THE VARIATION OF THE INTERNAL BALLISTICS OF A SOLID FUEL RAM-JET THROUGH COMBUSTOR DESIGN		5. TYPE OF REPORT & PERIOD COVERED Master's Thesis (September, 1973) 6. PERFORMING ORG. REPORT NUMBER
7. AUTHOR(s) Charles Ernest Jones, III		8. CONTRACT OR GRANT NUMBER(s)
9. PERFORMING ORGANIZATION NAME AND ADDRESS Naval Postgraduate School Monterey, California 93940		10. PROGRAM ELEMENT, PROJECT, TASK AREA & WORK UNIT NUMBERS
11. CONTROLLING OFFICE NAME AND ADDRESS Naval Postgraduate School Monterey, California 93940		12. REPORT DATE September, 1973 13. NUMBER OF PAGES 77
14. MONITORING AGENCY NAME & ADDRESS(if different from Controlling Office) Naval Postgraduate School Monterey, California 93940		15. SECURITY CLASS. (of this report) Unclassified 15a. DECLASSIFICATION/DOWNGRADING SCHEDULE

16. DISTRIBUTION STATEMENT (of this Report)

Approved for public release; distribution unlimited.

17. DISTRIBUTION STATEMENT (of the abstract entered in Block 20, if different from Report)

18. SUPPLEMENTARY NOTES

19. KEY WORDS (Continue on reverse side if necessary and identify by block number)

ramjet
solid fuel
recirculating flow
internal ballistics

20. ABSTRACT (Continue on reverse side if necessary and identify by block number)

An experimental investigation of the internal ballistics of solid fuel ramjets was conducted in order to more adequately define the pertinent variables in combustor design. The experimental investigation included the effects of wall mass addition on the recirculation zone of a rearward facing step combustor design, various methods of combustor flame stabilization, and the effects of inlet turbulence on the internal

DD FORM 1473 1 JAN 73 EDITION OF 1 NOV 65 IS OBSOLETE
(Page 1) S/N 0102-014-6601 |

20. (con't.)

ballistics of the combustor.

Flow conditions within the recirculation zone were unaffected by varying rates of wall mass addition.

Swirl devices and centerbodies were found to be inadequate substitutes for the rearward facing step inlet.

The solid fuel ramjet combustor was found to be highly susceptible to inlet turbulence. Smooth inlet ducting 45 degrees off centerline provided nearly identical flame stabilization characteristics and regression rates as that of a previously designed axial inlet configuration.